prestressed concrete institute

RESEARCH PROJECT NO. 5

DESIGN OF SPANDREL BEAMS

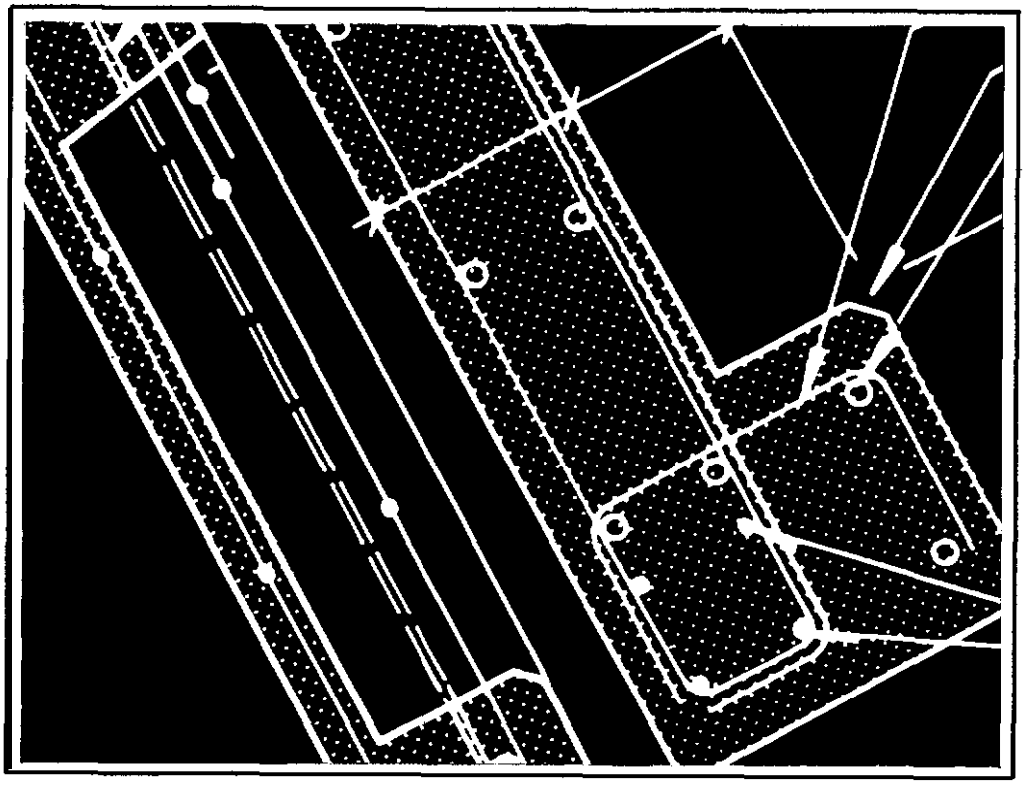

Wiss, Janney, Elstner Associates, Inc.
Northbrook, Illinois

SUPPORTING FIRMS

PCI SPECIALLY FUNDED R & D PROGRAM
Phase I-1982-1985

PRODUCER MEMBERS

Arnold Concrete Products
Baass Concrete Co.
Basalt Precast, A Division of Dillingham Heavy Construction, Inc.
Blakeslee Prestress, Inc.
Buehner Concrete Co.
Joseph P. Carrara & Sons, Inc.
Central Pre-Mix Concrete Co.
Colorado Concrete Structures, Inc.
Concrete Technology Corporation
Dura-Stress, Inc.
Everman Corporation
Exposaic Industries, Inc.
Fabcon Incorporated
Featherlite Corporation (Prestress Div.)
Finfrock Industries, Inc.
Florence Concrete Products, Inc.
Forest City Dillon Precast Systems, Inc.
Formigli Corporation
F-S Prestress, Inc.
Genstar Structures Limited
Heldenfels Brothers, Inc.
High Concrete Structures, Inc.
F. Hurlbut Company
Lone Star Industries, Inc.
Lone Star/San-Vel
Macon Prestressed Concrete Company
Material Service Corporation
Meekins-Bamman Prestress, Inc.
Metromont Materials Corporation
Morse Bros., Inc., Prestress Concrete Group
New Enterprise Stone & Lime Co., Inc.
Nitterhouse Concrete Products, Inc.
J. H. Pomeroy & Co., Inc.
Prestressed Concrete Operations
Price Brothers Co.
Rockwin Corporation
Rocky Mountain Prestress. Inc.
Shockey Bros., Inc.
Southeast Schokbeton, Inc.
Southern Prestressed Concrete, Inc.
Spancrete of California
Stanley Structures
Stresscon Corporation
Thomas Concrete Products Co.
Tindall Concrete Products, Inc.
TXI Structural Products, Inc.
The United Precasting Corporation
Universal Concrete Products Corporation
Wells Concrete Products Co.
Western American Concrete, Inc.

ASSOCIATE MEMBERS

American Spring Wire Corp.
American Steinweg Company, Inc.
Armco Inc.
J. I. Case Company
Dayton Superior Corporation
Dur-0-Wal. Inc.
Dy-Core Systems Inc.
Elkem Chemicals, Inc.
Fehr Brothers, Inc.
Florida Wire&Cable Co.
Forton PGFRC, Inc.
Hamilton Form Company, Inc.
Martin Marietta Cement
Mi-Jack Products
Mixer Systems, Inc.
Ted Nelson Company
Plant City Steel Company
Prestress Supply, Inc.
Spillman Company
Springfield Industries Corp.

PROFESSIONAL MEMBERS

ABAM Engineers, Inc.
W. Burr Bennett Ltd.
Ross Bryan Associates, Inc.
Conrad Associates East
The Consulting Engineers Group, Inc.
Langstrand Associates. Inc.
LEAP Associates International, Inc.
Irwin J. Speyer
H. Wilden &Associates, Inc.
Wiss, Janney, Elstner Associates, Inc.

Specially Funded R & D Program

Research Project No. 5

DESIGN OF SPANDREL BEAMS

Gary J. Klein

Wiss, Janney, Elstner Associates, Inc.

330 Pfingsten Road

Northbrook, IL 60062

STEERING COMMITTEE

Ned M. Cleland, Chairman

Alex Aswad
John Bachman
Ken Baur
Kamal Chaudhari
Keith Gum
John Hanlon
Floyd Jones
Stuart McRimmon
Joseph A Miller
Kim E. Seeber
C. P. Siess (RCRC)
Robert Smith
Tom A. Thomas, Jr.
Garry Turner

EXECUTIVE SUMMARY

The behavior and design of precast spandrel beams was studied under PCISFRAD Project #5. This research project was primarily directed toward spandrel beams commonly used in parking structures. Both L-beams and pocket spandrels were included in the study.

The research included background investigation of design practices, analytical studies using finite element models, and full-scale load tests of two L-beams and one pocket spandrel. All three test specimens were 72 in. high, 8 in. wide and 28 ft long. The target design loads were based on 90 psf dead load and 50 psf live load, which are typical for a double tee parking structure with 60 ft spans.

The background research revealed that industry practices and published procedures vary with respect to several fundamental aspects of spandrel beam design. Behavior near the end regions is not well understood, nor is the influence of connections to deck elements. In general, the design of beam ledges is not consistently handled; in particular, there is no consensus on the design of hanger reinforcement for ledge-to-web attachment. Also, the ACI Building Code (ACI 318-83) does not address combined sheer and torsion in prestressed beams. Designers rely on several research reports that give design recommendations.

Ledge-to-web attachment and behavior near the end region of spandrels were identified as the key issues and were the primary focus of this research. The analytical studies and laboratory testing program yielded several significant findings:

- Contrary to several published design examples, a critical section for shear and torsion at the face of the support should be considered.
- Connections to deck elements do not substantially reduce torsion: however, they are effective in restraining lateral displacement induced by bending about the weak principal axis.
- Shear and torsion design procedures for prestressed spandrels which consider a concrete contribution have been verified by two tests.

- An approach for considering the effect of the pocket on the shear strength of pocket spandrels has been proposed. While the accuracy of this approach has not been fully verified by tests, it is believed to be conservative.
- With regard to detailing practices. it was found that the torsional response of deep spandrels is dominated by out-of-plane bending. The use of lapped-splice stirrups and longitudinal reinforcing bars without hooks does not appear to have any detrimental effect.
- Two independent design checks in the end region of spandrels are recommended. First, reinforcement should be provided to resist out-of-plane bending caused by the horizontal torsional equilibrium reactions. This reinforcement is not additive to the reinforcement for internal torsion. Second, the longitudinal reinforcement in the bearing area should be sufficiently developed to resist the external normal force, as well as the tension induced by the vertical reaction.
- The eccentricity of the ledge load cannot be neglected in the design of hanger reinforcement for ledge-to-web attachment. Nonetheless, not all of the load acting on the ledge is suspended from the web and the effective eccentricity of the ledge load is significantly reduced due to torsion within the ledge. A design procedure which considers these effects has been recommended. In addition. it wss determined that hanger reinforcement is not additive to shear and torsion reinforcement.
- The PCI design equations for punching shear strength of beam ledges may be unconservative. Further research in this ares is recommended.

In conclusion, this research has clarified many of the questions relating to spandrel beam design and the design recommendations will be of immediate benefit to the precast industry.

TABLE OF CONTENTS

1. INTRODUCTION

Spandrel beams are one of the most complex elements in precast construction. Industry practices and published procedures vary with respect to several fundamental aspects of their design. Behavior near the end region is not well understood, nor is the influence of connections to deck elements. I" general, the design of beam ledges is not consistently handled; in particular, there is no consensus on the design of hanger reinforcement for ledge-to-web attachment. A1so, the ACI Building Code (ACI 318-83)[1] does not address combined shear and torsion in prestressed beams, although several research reports give design recommendations.

PCI Specially Funded Research and Development Project #5 addressed these issues by studying the behavior and design of precast spandrel beams. The research program was primarily directed toward deep and slender spandrels such as those commonly used in parking structures to serve both load-carrying and railing functions. Both L-beams and spandrel beams with pockets for T-stem bearings (pocket spandrels) were included in the program. Figure 1.1 shows typical cross sections of these types of beams. The findings of this research generally apply to both prestressed and non-prestressed spandrels, but may *not* be applicable to spandrel beams of radically different geometric configuration or load level. Furthermore, while this research is believed to be reasonably comprehensive, not all aspects of spandrel beam design are covered. In particular, the research does not address spandrel beam design as part of a lateral-load-resisting frame, "or the effects of volume change on design and detailing of spandrels. Also, handling and vehicular impact loads are not discussed. These considerations can be very important, but are considered beyond the scope of this research.

The research included the following:

- Study of design requirements and practices to determine the state-of-the-art of spandrel beam design.
- Analytical studies using finite element models of a" L-beam and pocket spandrel.
- Full-scale tests of two L-beams and one pocket spandrel designed using state-of-the-art methods.

The following sections of this report describe the research. analyze the findings, and provide design recommendations.

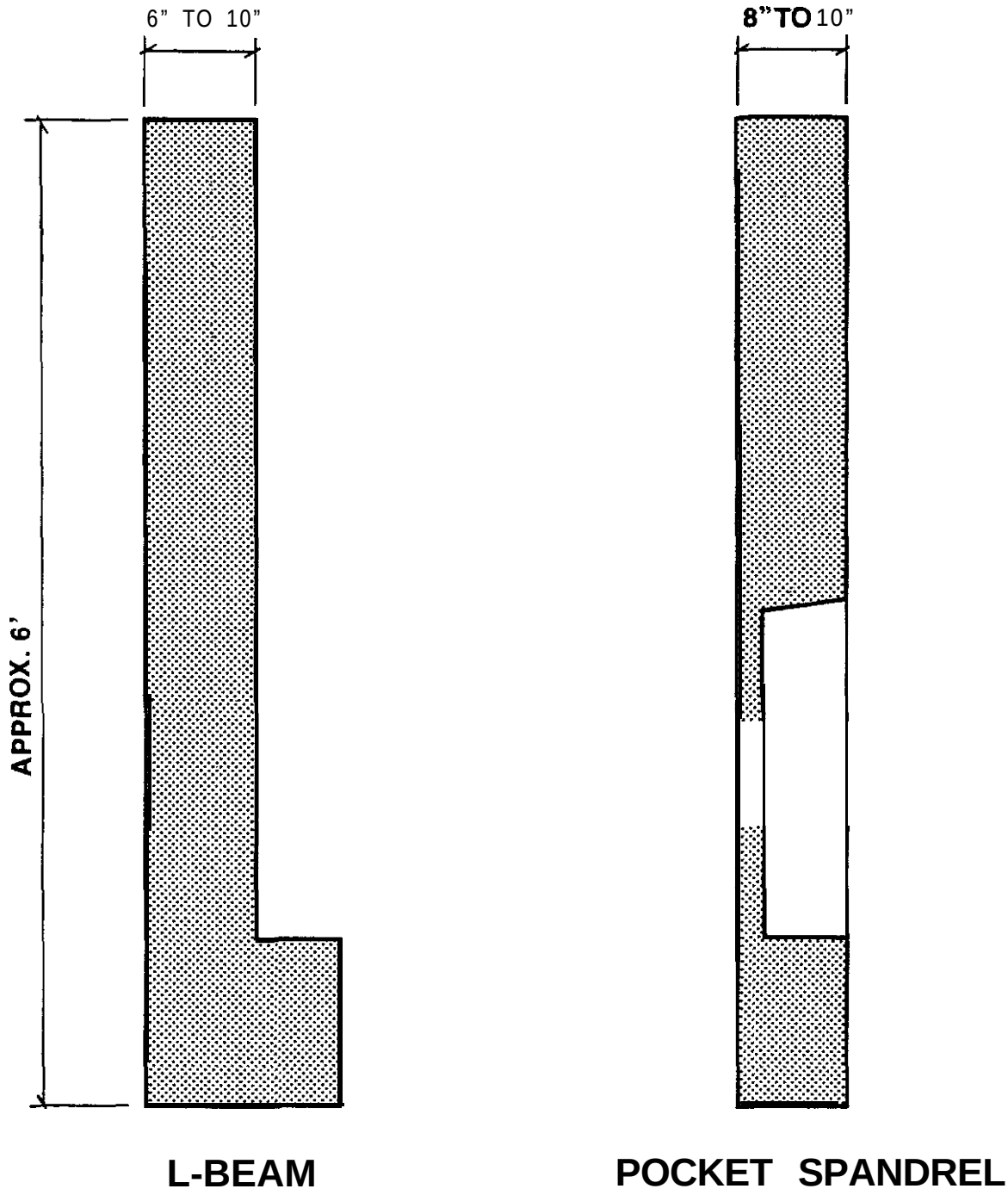

Fig. 1.1 – Typical spandrel sections

2. BACKGROUND RESEARCH

The background research included a review of code requirements, published guides and research reports on spandrel beam design. A questionnaire covering several aspects of spandrel beam design was sent to the members of the Steering Committee for PCISFRAD Project #5. Later, a questionnaire on pocket spandrels was sent to selected committee members who showed interest in that type of construction. Finally, the collective experience of the author and his associates was considered. The following discussion on spandrel beam design is based on this research.

2.1 General Design Considerations

Critical section. In most precast beams, the loads and reactions are applied at the top and bottom of the beam, respectively. Such beams are said to be "directly loaded". Spandrel beams, on the other hand, are indirectly loaded, and the additional shear capacity due to arch action near the support is not available.[2] Therefore, design for shear and torsion forces at a distance d (h/2 for prestressed spandrels) from the support may be not appropriate. Figure 2.1 shows potential critical inclined sections which carry all the concentrated loads acting on the ledge rather than just loads farther than d from the support.

The consensus among designers is that all loads acting on the ledge inside the critical section, based on inclined cracking from the edge of the beam base plate. must be considered as part of the shear/torsion load. This consensus is contrary to the published design examples in Section 4.4 of the PCI Design Handbook[3] and Example 14.2 in the PCA notes on ACI 318-83.[4] ACI 318-83 does not address indirectly loaded beams; however, Article 11.1.2 of the Commentary recommends special consideration for concentrated loads near supports.

Equivalent uniform load. It is common practice to simplify the analysis by replacing concentrated loads with equivalent uniform loads. Some designers increase the equivalent uniform floor load such that the shear and torsion is correct at the critical section at the inside edge of the base plate i.e., the basic equivalent uniform load is multiplied by the ratio of grid span to design span.

Eccentricity contributing to torsion. Typically, the ledge loads are positioned at the centerline of bearing (allowing for fabrication and erection tolerances) or at the outer 1/4 point of the ledge. The former approach is generally preferred because an increase in ledge projection does not necessarily require an increase in torsional load. The eccentricity contributing to torsion is the distance from the centerline of the web to the applied load, as shown in Fig. 2.2. Theoretically, the eccentricity should be measured relative to the shear center. which, for an uncracked L-beam section, is slightly inside the centerline of the web. However, this difference is neglible in deep spandrels. Further, experimental results are not consistent with the theoretical prediction of shear center location based on the uncracked cross section.[5]

Influence of deck connections. Prior to connection of the double tees or topping to the spandrels, torsion can be computed as a product of the dead load and the eccentricity between the applied load and centerline of the web. After connections to deck elements are made, however, the applied "live load" torsion may be partially counteracted by the horizontal force due to friction at the bearing pads coupled with restraint at the deck connections (Fig. 2.2). However, most practitioners believe that it is inappropriate to rely on a soft bearing pad for this purpose. In addition. recent research[6] indicates that the effective "friction" at the bearing pad may be 5 percent or less of the gravity load.

2.2 Flexure

Flexural design of spandrels generally follows ACI and PCI procedures for bending about the horizontal and vertical axes. However, L-shaped spandrel beams do not have symmetry about either axis. The principal axes are rotated‘slightly from the vertical and horizontal axes, as shown in Fig. 2.3. The influence of this rotation on bending about the horizontal axis can be neglected for deep spandrel beams. For shallow spandrels. particularly those employing prestressing, this influence should be considered.

Perhaps more important, however, is the influence of principal axes rotation on horizontal displacement of spandrels. As shown in Fig. 2.3, a component of the vertical load acts along the weak axis inducing

a" outward horizontal displacement. All loading prior to making diaphragm connections can cause horizontal displacement. Cleland[5] found that this was the most dominant behavior of long slender spandrels and suggests a principal axes analysis when the spa" length is 40 to 50 times web width, depending on the intermediate support conditions.

I" general, detailing practice follows the ACI code. One noteworthy exception pertains to Article 10.6.7 of the ACI 318-83 which is applicable to non-prestressed spandrels. This provision requires that reinforcement be placed in the side faces of webs more than 3 ft deep. The reinforcement is to be distributed in the zone of flexural tension with a spacing not more than the web width, nor 12 in. Designers do not often check this provision; instead reinforcement in the side faces of the web is designed to resist torsion or handling.

2.3 Shear and Torsion

Prestressed spandrels. The ACI code does not address torsion in prestressed concrete. A procedure for torsion design of prestressed concrete, which is a" extension of the ACI provisions of torsion for non-prestressed concrete. was developed by Zia and McGee.[7] The second edition of the PCI handbook included a modified version of the Zia and McGee method.[8] The PCI procedure uses a simplified method for computation of torsional stress which is conservative for most spandrel beams. A further refinement of these methods was subsequently developed by Zia and Hsu.[9] While the general design approach follows that of Zia-McGee and PCI, new expressions are proposed for torsion/shear interaction and minimum torsion reinforcement. The Zia-Hsu equations are expressed in terms of forces and moments rather than nominal stresses, which is more consistent with the current ACI code.

Most designers follow one of these three similar procedures. Practices vary with respect to the design of longitudinal reinforcement for torsion. Some designers consider the prestressing strand to be part of the longitudinal reinforcement while others consider only the mild reinforcing. In their original paper. Zia and McGee recommended that only the prestressing steel in excess of that required for flexure, and located

around the perimeter of closed stirrups. should be considered as part of the longitudinal torsion steel.

The third edition of the PCI handbook[3] describes a procedure developed by Collins and Mitchell, which is based on compression field theory. This approach assumes that, after cracking, the concrete can carry no tension and that shear and torsion are carried by a field of diagonal Compression. Because' the "concrete contribution" is neglected, this approach will generally require somewhat more stirrup reinforcement depending on the selection of the crack angle. The biggest difference, however, is in the positive and negative moment capacity requirements which are based on the axial tension caused by shear and torsion. For the example shown, in the handbook, the required positive and negative bending strength at the face of the support exceeds the midspan moment. These requirements present considerable detailing difficulties, and many designers do not feel they are valid for deep spandrels.

Detailing practices for the torsional reinforcement do not always follow ACI code requirements. Article 11.6.7.3 requires that transverse reinforcement consist of closed stirrups, closed ties or spirals. However, the'commentary to the ACI code indicates that this requirement is primarily directed 'at hollow box sections and solid sections subjected primarily to torsion. In these members, the side cover spalls off, rendering lapped-spliced stirrups ineffective. This type of behavior is unlikely in deep spandrel beams, and transverse reinforcement is often provided by pairs of lapped-spliced U-stirrups. Also, most designers feel that the stirrup spacing limit of 12 in. is not appropriate for deep spandrels, and this limit is routinely exceeded.

Non-prestressed spandrels. Torsion design of non-prestressed concrete generally follows ACI code requirements, except for the detailing considerations discussed above.

Pocket spandrels. Typically, pocket spandrels need not be designed for torsion. However, the pockets complicate the shear design. Design practices vary for considering the effect of the pocket; some designers neglect this effect. Fortunately, shear strength does not control the dimensions of deep pocket spandrels and often only minimum reinforcement is required. Welded wire fabric is frequently used for web reinforcement.

2.4 Beam End Design

Torsion equilibrium. The eccentric load applied on the ledge produces torsion in the spandrel which must be resisted by reactions at the supports. Customarily. the web is connected to the column to restrain rotation. Figures 2.4a and 2.4b show the torsion equilibrium reactions for a normal and dapped connection, respectively.

The torsional equilibrium reactions may require supplemental vertical and horizontal web reinforcement at the ends of the girder. Raths[10] and Osborn[11] prescribe similar methods for design of this reinforcement. Vertical and longitudinal steel, A_{wv} and $A_{w\ell}$, on the inside face of the spandrel is calculated by:

$$A_{wv} = A_{w\ell} = \frac{T_u}{2\phi f_y d_s} \qquad (1)$$

where T_u = factored torsional moment at the end of girder (in-lbs),
d_s = depth of A_{wv} and $A_{w\ell}$ steel from outside face of spandrel (in.),
f_y = yield strength of reinforcement (psi) (or effective prestress),

and ϕ = strength reduction factor = 0.85.

The use of ϕ = 0.85 instead of 0.90 (flexure) compensates for the ratio of internal moment to total effective depth, which is not in Equation 1.

Osborn recommends the bars be evenly distributed over a height and width equal to h_s (see Fig. 2.4) from the concentrated reaction point.

Because shear cracks may coincide with diagonal cracks due to out-of-plane bending, A_{wv} should be added to the shear reinforcement. However, most designers feel this reinforcement is not additive to reinforcement for internal torsion. If the reinforcement for torsion is considered to function as A_{wv} and $A_{w\ell}$ reinforcement, little or no supplemental reinforcement is required provided all loads acting on the ledge are considered as part of the shear/torsion load.

Figure 2.5 shows a" alternative means to provide torsional equilibrium at the support. I" this case, the end reactions are in close alignment with the ledge loads. The projecting beam ledge is treated as an upside-down corbel. Most designers surveyed indicated that this approach may lead to *excessive* rolling of the spandrel beam at the support, particularly where a soft bearing pad is used.

Dapped-end beams. Section 6.13 of the PCI Design Handbook presents design criteria for dapped-end connections. Research on dapped connections under PCISFRAD Project #6, which is being conducted concurrently with this project, is expected to recommend modified procedures. Design of dapped end L-beams is often complicated by reinforcement for torsion equilibrium connections (Fig. 2.4b). Also, the last blockout in a pocket spandrel often interferes with the reinforcing for the dapped end. The established design procedures are modified as appropriate to handle these special conditions.

2.5 Beam Ledges

Hanger reinforcing. Figure 2.6 illustrates a possible separation between the ledge and web of a" L-shaped spandrel. Design examples by PCA[4] and Collins and Mitchell[12] provide hanger reinforcement concentrated near the ledge load given by

$$A_{sh} = \frac{V_u}{\phi f_y} \qquad (2)$$

The notation is defined below.

Raths[10] uses all the hanger reinforcement between ledge loads, but computes the required reinforcement based on the summation of moments about the outside face of the spandrel, thus

$$A_{sh} = \frac{V_u}{\phi f_y} \frac{(jd+a)}{jd} \qquad (3)$$

where A_{sh} = area of transverse hanger reinforcement on inside face of spandrel for each ledge load (sq in.).

V_u = factored ledge load (kips),

a = distance from ledge load to center of inside face reinforcement (in.),

jd = internal moment arm (in.) (taken as d - 1/2 in.).

and ϕ = strength reduction factor = 0.85.

Raths recommends an additional load factor of 4/3 for design of hanger reinforcement. An alternate procedure for using concrete tension as a means of ledge-to-web attachment is also given.

Equation 3 is based on sound principles of statics, yet there are many existing spandrels that have performed well with much less reinforcement than this equation would require. The only known failures have occurred where there was no hanger reinforcement. In several instances, beams with very light hanger reinforcement have survived load tests.

Further refinements of hanger reinforcement design[11,12,13] reduce the load that must be suspended from the web based on internal shear stress distribution, relative depth of the ledge, and deflection compatibility.

There is no consensus among designers on requirements for hanger reinforcement. Some designers do not check ledge-to-web attachment, while others use some combination of the above methods. Furthermore, there is no agreement as to whether or not hanger reinforcement should be added to shear and torsion reinforcement. The method for designing hanger reinforcement generally controls the quantity of transverse reinforcement in the middle region of the spandrel, and can have a very significant effect on material and fabrication costs.

Ledge punching shear. The design for punching shear in beam ledges generally follows the procedures in Section 6.14 of the PCI Handbook.

Some designers follow a modified procedure recommended by Raths;[10] based on unpublished test results, this method considers a lower ultimate stress on the vertical shear plane along the inside face of the web. Mirza, et al[14] and Krauklis and Guedelhofer[15] have also found that the PCI design equations may be unconservative.

2.6 Beam Pockets

It is customary to provide closed stirrups or U-bars in the plane of the web for the entire T-stem load in pocket spandrels. The hanger bars are typically located near the T-stem load, as shown in Fig. 2.7. Therefore, Equation 2 is used to determine hanger reinforcement requirements. The concrete tensile stress at the "ledge" level is relatively low so a horizontal crack at that location is unlikely. Also, because hanger reinforcement is customarily used, punching shear below the pocket is generally not a concern.

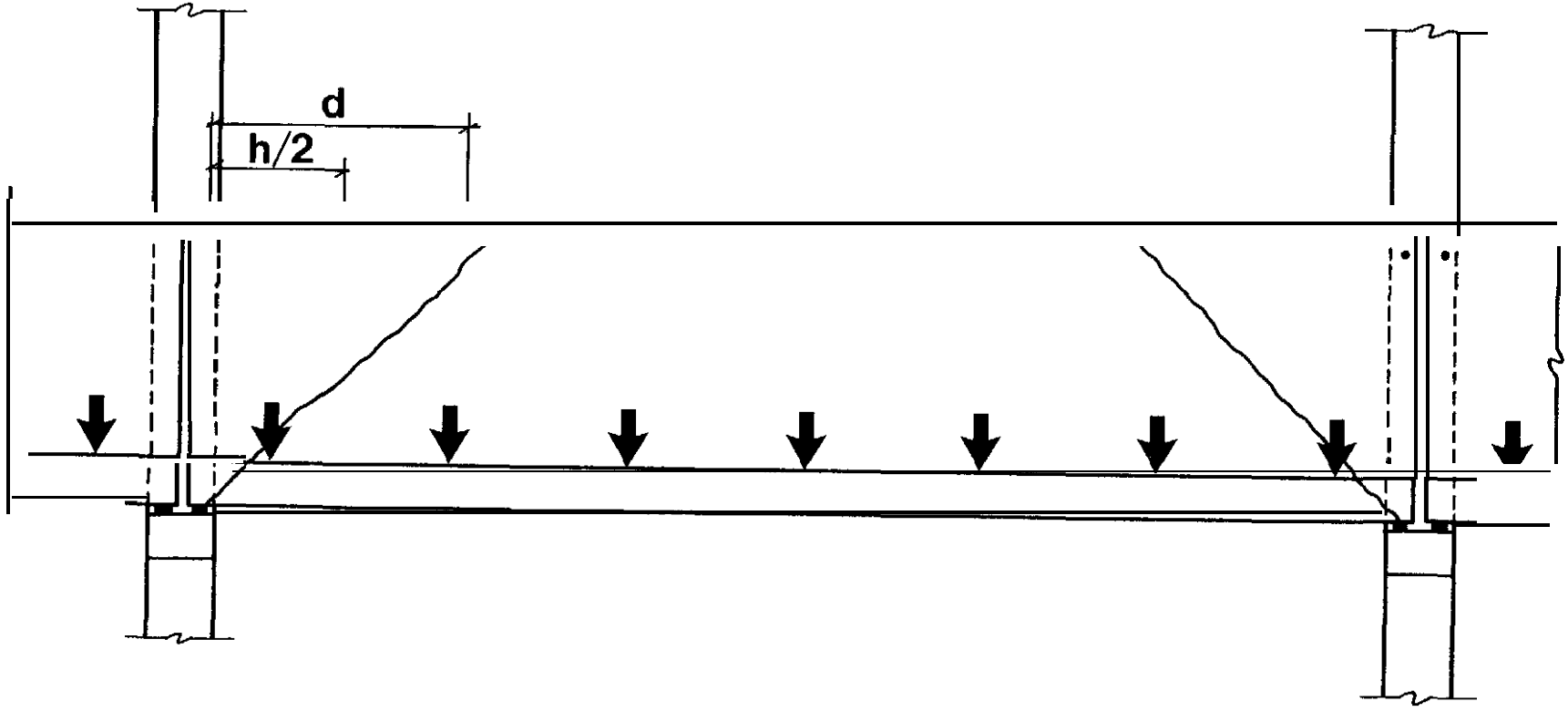

Fig. 2.1 - Critical inclined sections in an "indirectly loaded" spandrel

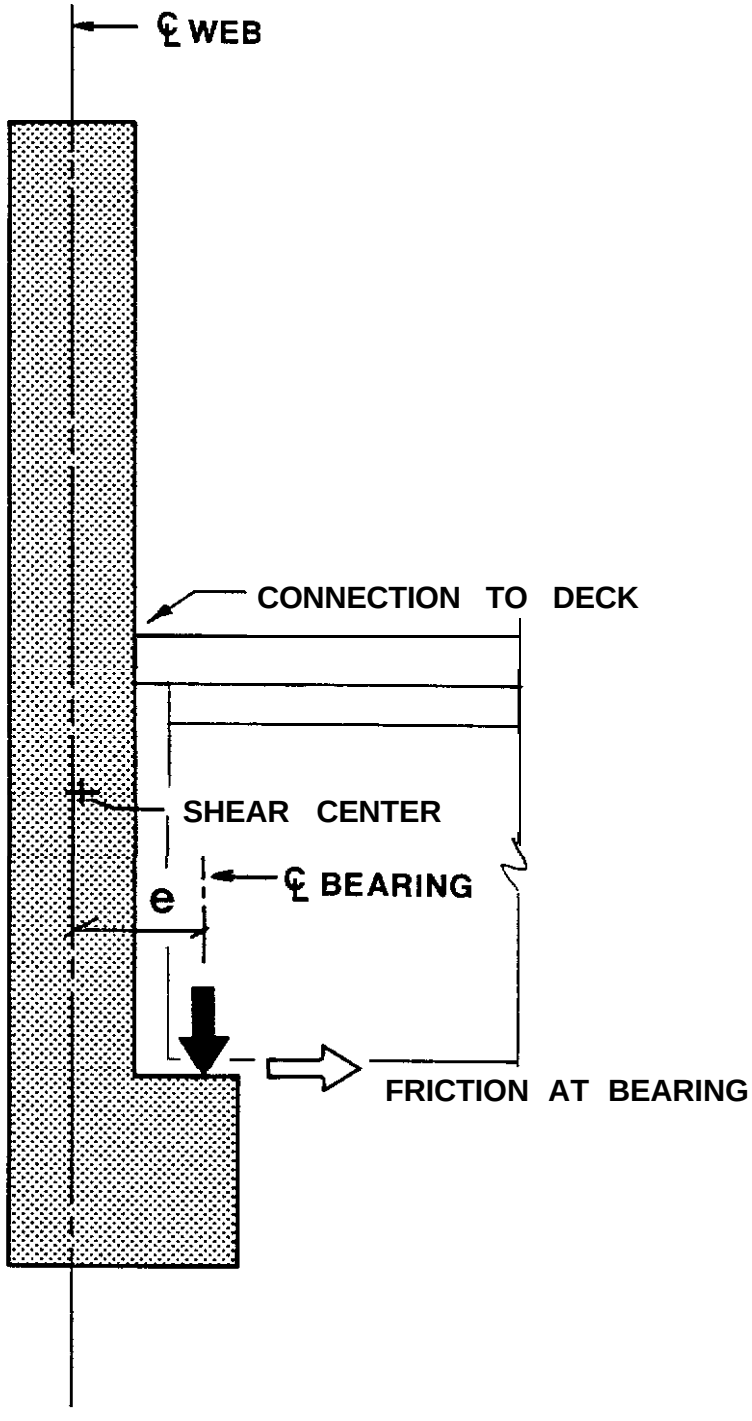

Fig. 2.2 – Eccentricity contributing to torsion

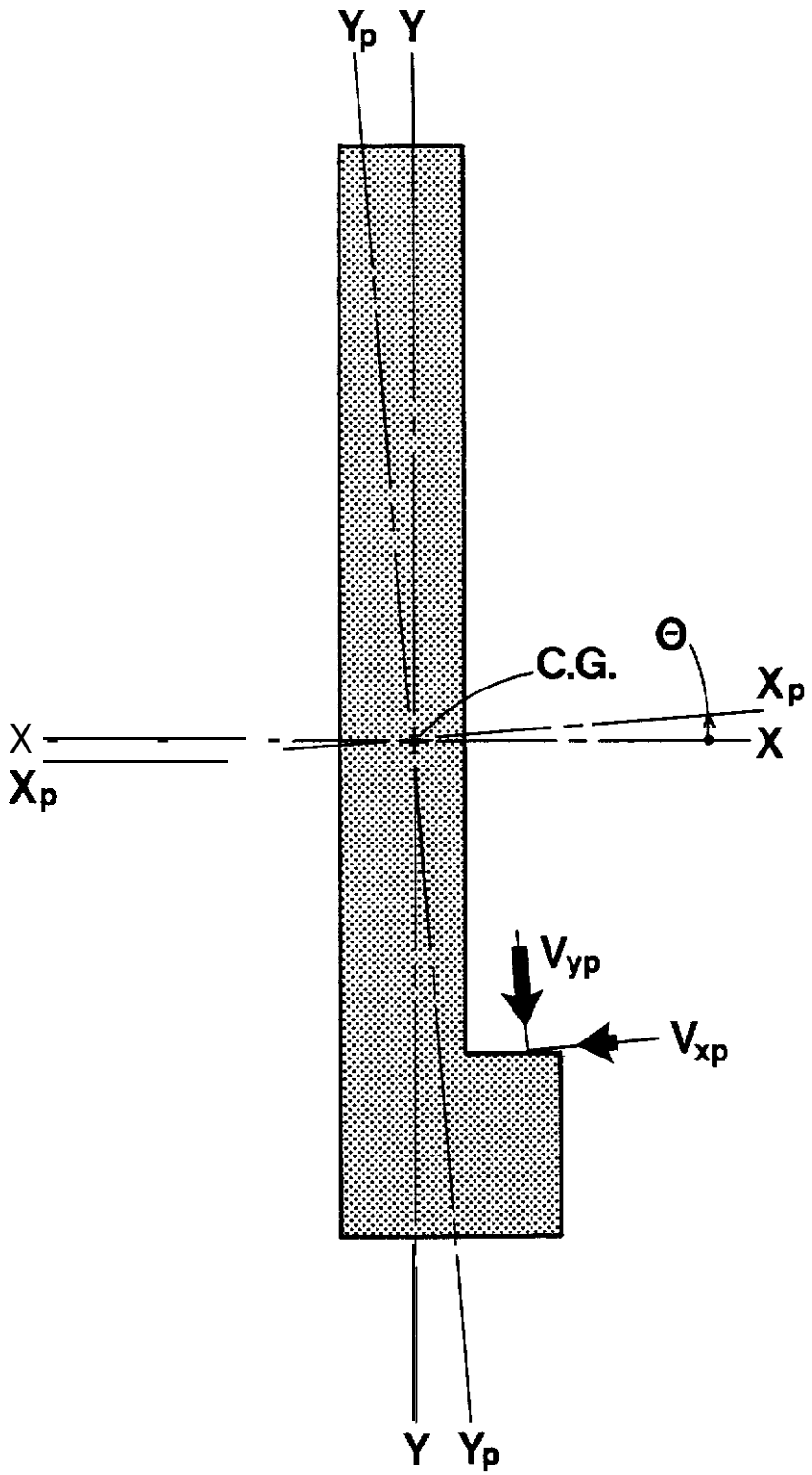

Fig. 2.3 - Principal axes of an L-beam

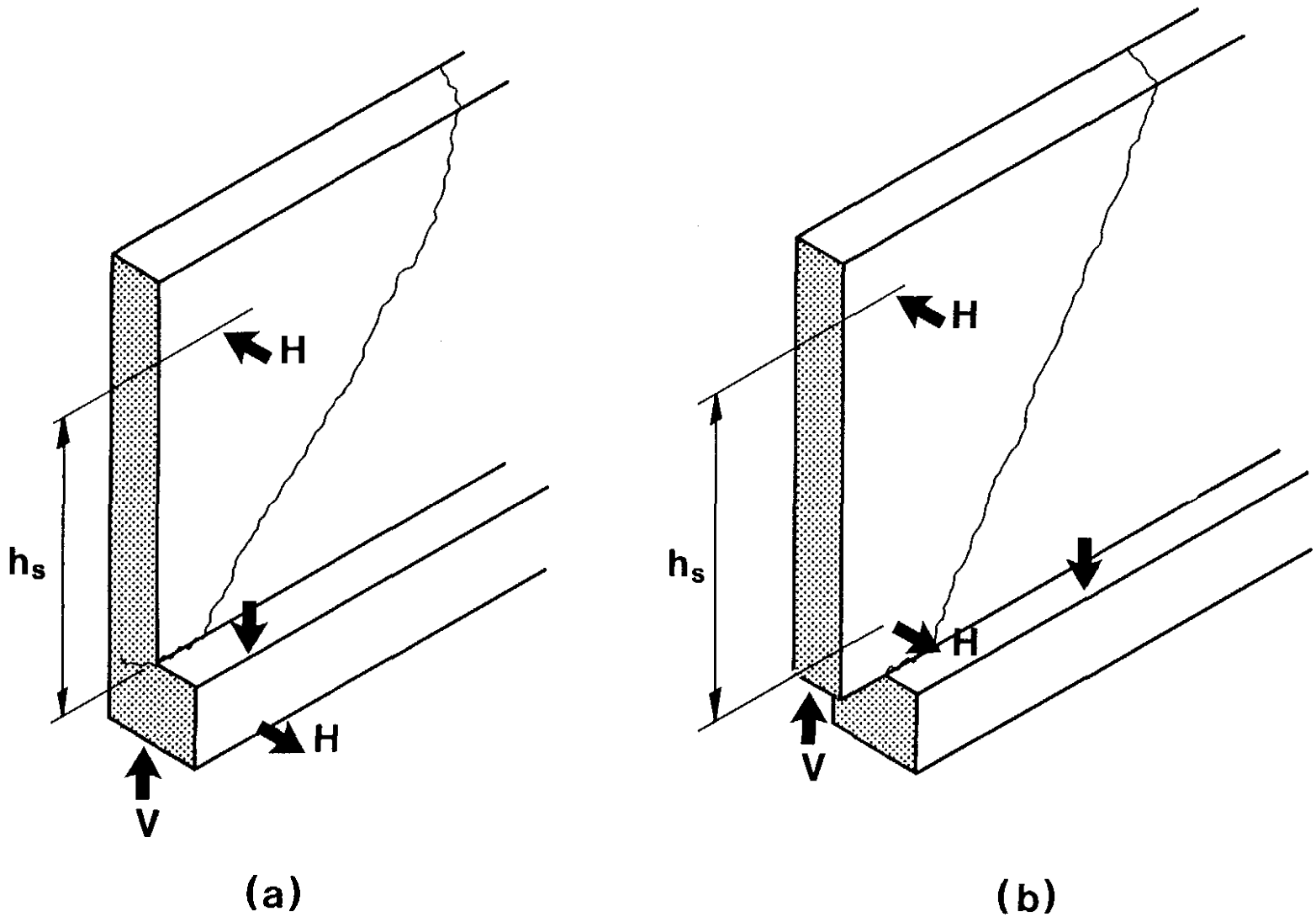

Fig. 2.4 Torsion equilibrium reactions

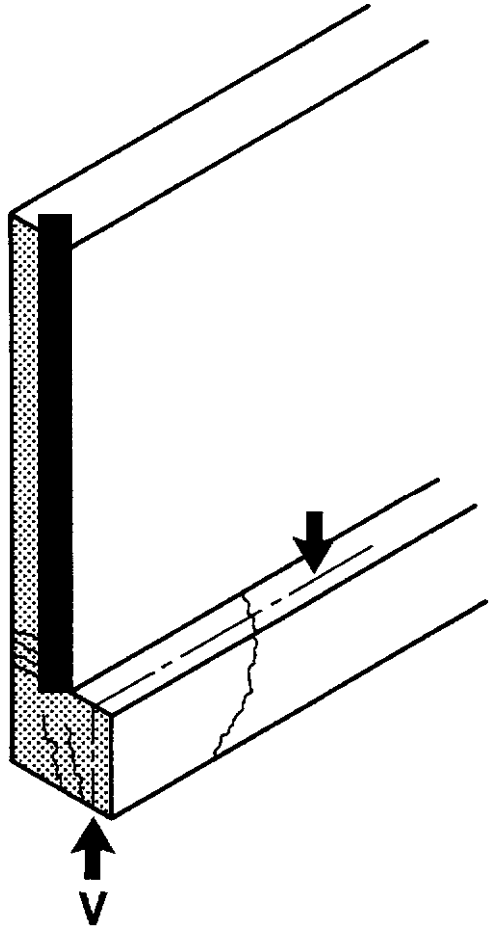

Fig. 2.5 – Beam end corbel behavior

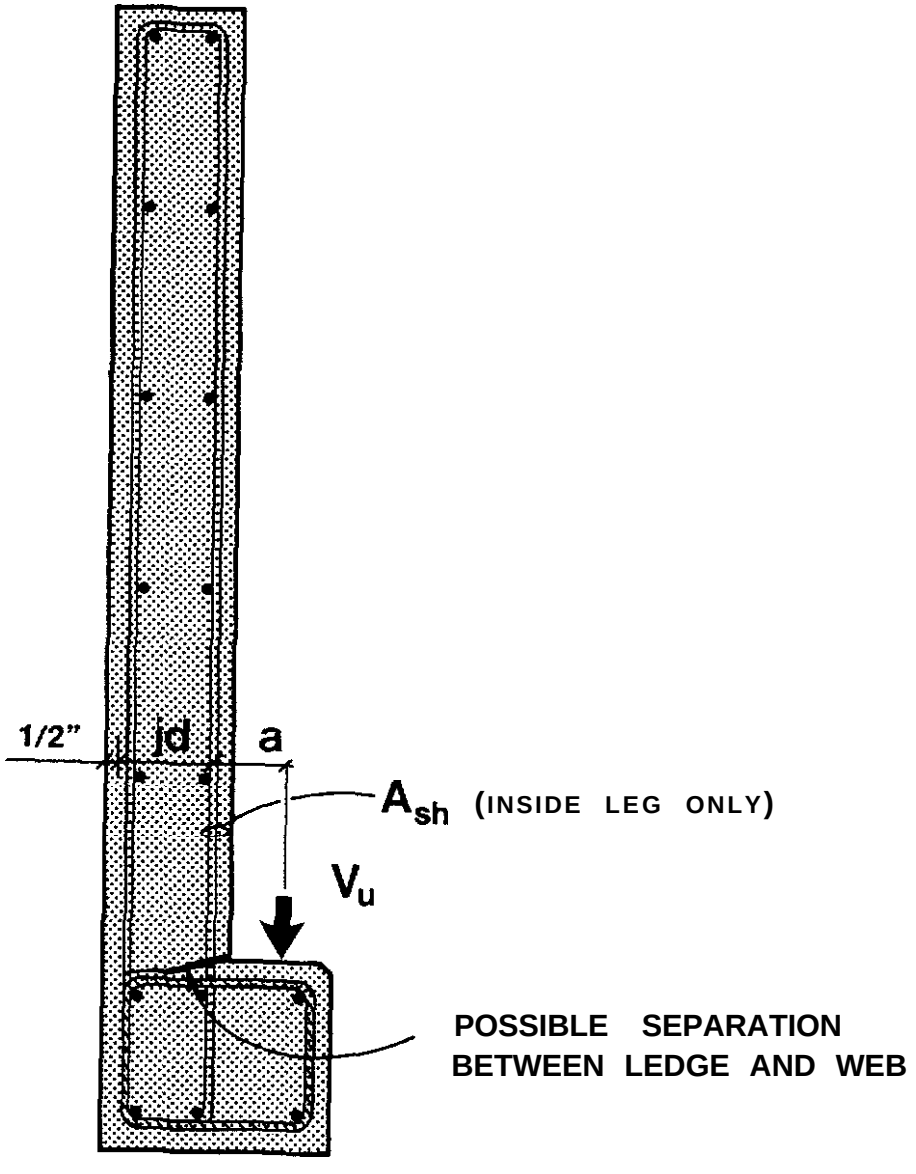

Fig. 2.6 – Ledge-to-web attachment

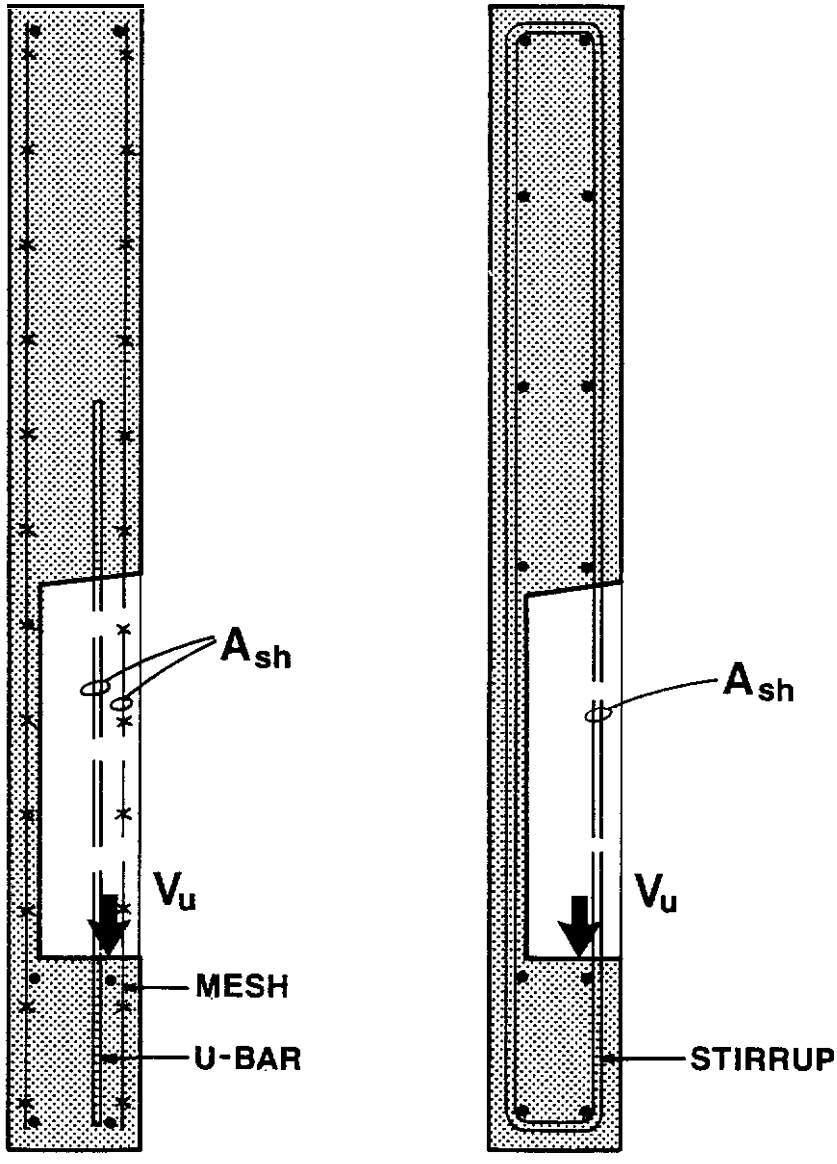

Fig. 2.7 – Hanger reinforcement in pocket spandrels

3. FINITE ELEMENT MODEL STUDIES

3.1 Description

Finite element models of a" L-beam and pocket spandrel were analyzed. The geometry of these models and the test specimens was essentially the same. The beams were 72 in. deep, 8 in. wide and 28 ft long. Figures 4.1 and 4.2 provide more detailed information on the geometry of the beams.

The model studies had several objectives:

- Investigate the deflections and rotations caused by the eccentrically applied load.
- Determine the theoretical torsional equilibrium reactions at the supports.
- Study the influence of connections to deck elements on deformations and torsional equilibrium reactions.
- Investigate the stresses across the ledge/web interface.

Three-dimensional solid elements were used with three degrees of freedom at each node. Cross sections showing the finite element mesh are shown in Figs. 3.1 and 3.2. The models were assembled and analyzed using a proprietary version of the SAP IV Program.

Service loads included beam dead load and a 16.8 kip tee-stem reaction at 4 ft centers. The tee-stem load was applied at 8 in. and 2 in. from the web centerline for the L-beam and pocket spandrel, respectively. The restraints at each end of the beam modeled a typical spandrel beam support where the bearing pad is placed at the centerline of the web, and lateral support is provided near the bearing and at the top corners of the beam.

For both the L-beam and pocket spandrel, a second condition was analyzed in which additional lateral restraint was provided near mid-height of the beam to simulate connections to deck elements. There was no possibility of relative lateral movement between the column restraints and deck elements, simulating the case where there is an independent connection between the deck and the column. This case was modeled so the analytical studies and load tests modeled the same condition, although it should be noted that a direct connection between the column and deck is not

necessarily required. Alternately, the column can be indirectly connected to the deck through the spandrel beam.

3.2 Spandrel Beam Behavior

Figure 3.1a shows the midspan deflection of the L-beam at service load without any connections to deck elements. Note the overall outward deflection due to the rotation of the principal axes. Connections to deck elements effectively restrain this outward displacement, as shown in Fig. 3.1b. Usually these connections are not made until all of the dead load is in place, Similar plots for the pocket spandrel are shown in Fig. 3.2. Due to the different cross-sectional shape and load eccentricity, the lateral deflection is relatively small.

Figure 3.3a shows the horizontal reactions at the L-beam support without connections between the spandrel and deck. These forces simply balance the external torsion due to the eccentrically-applied loads. Figure 3.3b shows the horizontal reactions with deck connections. The deck connections in the midspan region restrain the outward displacement. The deck connections at the support work with the top corner connections to restrain rotation. The net outward force between the deck and spandrel would be counteracted by the column-to-deck connection. If there were no column-to-deck connection, the deck connection forces would tend to balance. depending on the stiffness of the column.

3.3 Transfer of Ledge Loads to Web

Stresses across a plane 3 in. above the ledge/web interface were studied. (The geometry of the finite element mesh prevented investigation at the top of the ledge). The results of that study are presented in Fig. 3.4. As expected, the inside face of the web is in tension. The maximum tensile stress of 295 psi, which occurs at the ledge load, is about 40 percent greater than the average stress. The compression in the outside face of the web is significantly more uniform.

The resultant of these stresses can be computed by integrating stresses in the individual elements near the ledge/web junction. As indicated in the figure, the resultant is slightly less than the applied

ledge load and is shifted significantly towards the web centerline. These differences are equilibrated by shear and torsion in the ledge itself. This mechanism is discussed further in Section 5.4.

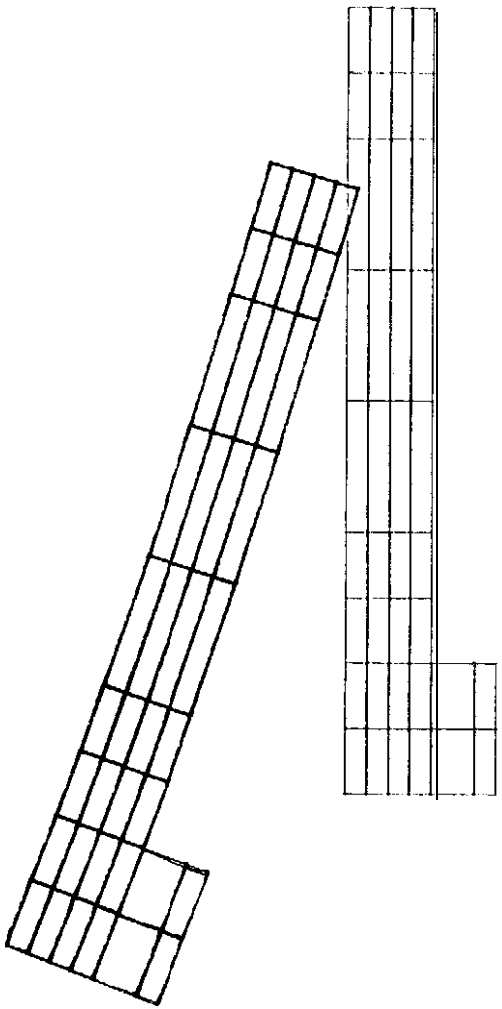

		F.E. MODEL	LOAD TESTS
VERT.	(IN.)	-0.060	-0.123
HORIZ.	(IN.)	-0.089	-0.094
ROT.	(RAD)	-0.00163	-0.00319

(A) WITHOUT DECK CONNECTIONS

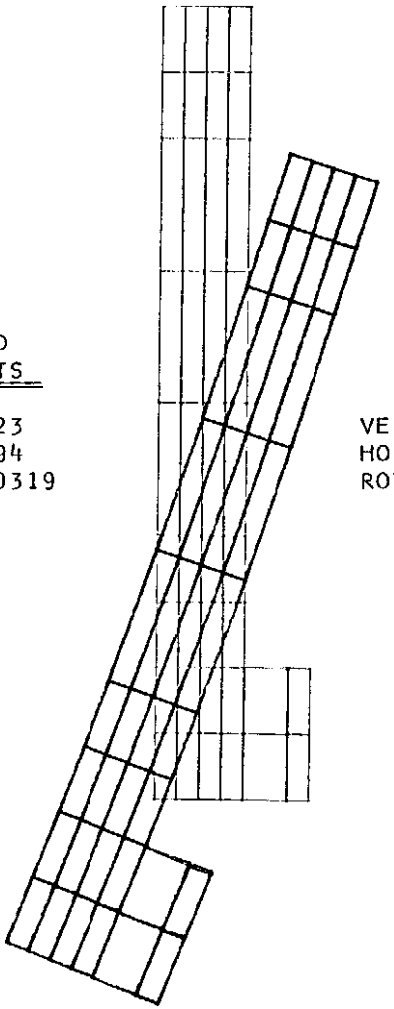

		F.E. MODEL	LOAD TESTS
VERT.	(IN.)	-0.056	-0.131
HORIZ.	(IN.)	-0.008	-0.057
ROT.	(RAD)	-0.00169	-0.00282

(B) WITH DECK CONNECTIONS

Fig. 3.1 - Midspan deflection of L-Beam (superimposed dead load plus live load)

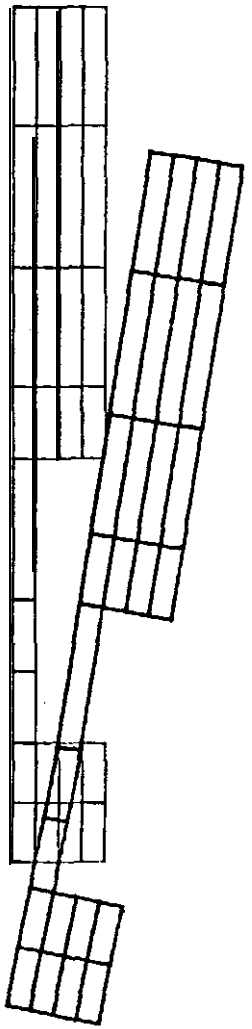

		F.E. MODEL	LOAD TESTS
VERT.	(IN.)	-0.053	-0.173
HORIZ.	(IN.)	+0.024	+0.038
ROT.	(RAD)	-0.00085	-0.00443

(A) WITHOUT DECK CONNECTIONS

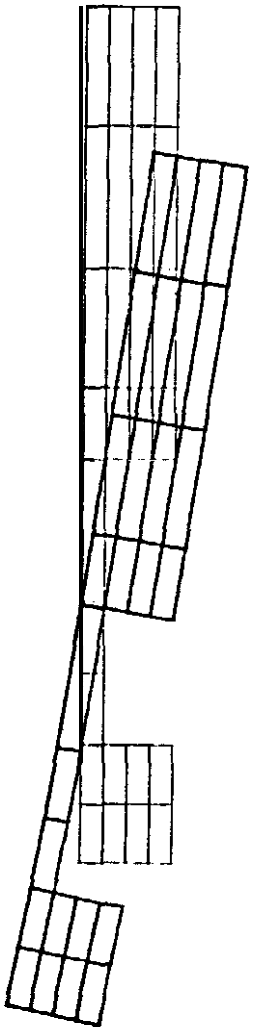

		F.E. MODEL	LOAD TESTS
VERT.	(IN.)	-0.053	-0.146
HORIZ.	(IN.)	0.0	+0.013
ROT.	(RAD)	-0.00083	-0.00346

(B) WITH DECK CONNECTIONS

Fig. 3.2 - Midspan deflection of pocket spandrel (superimposed dead load plus live load)

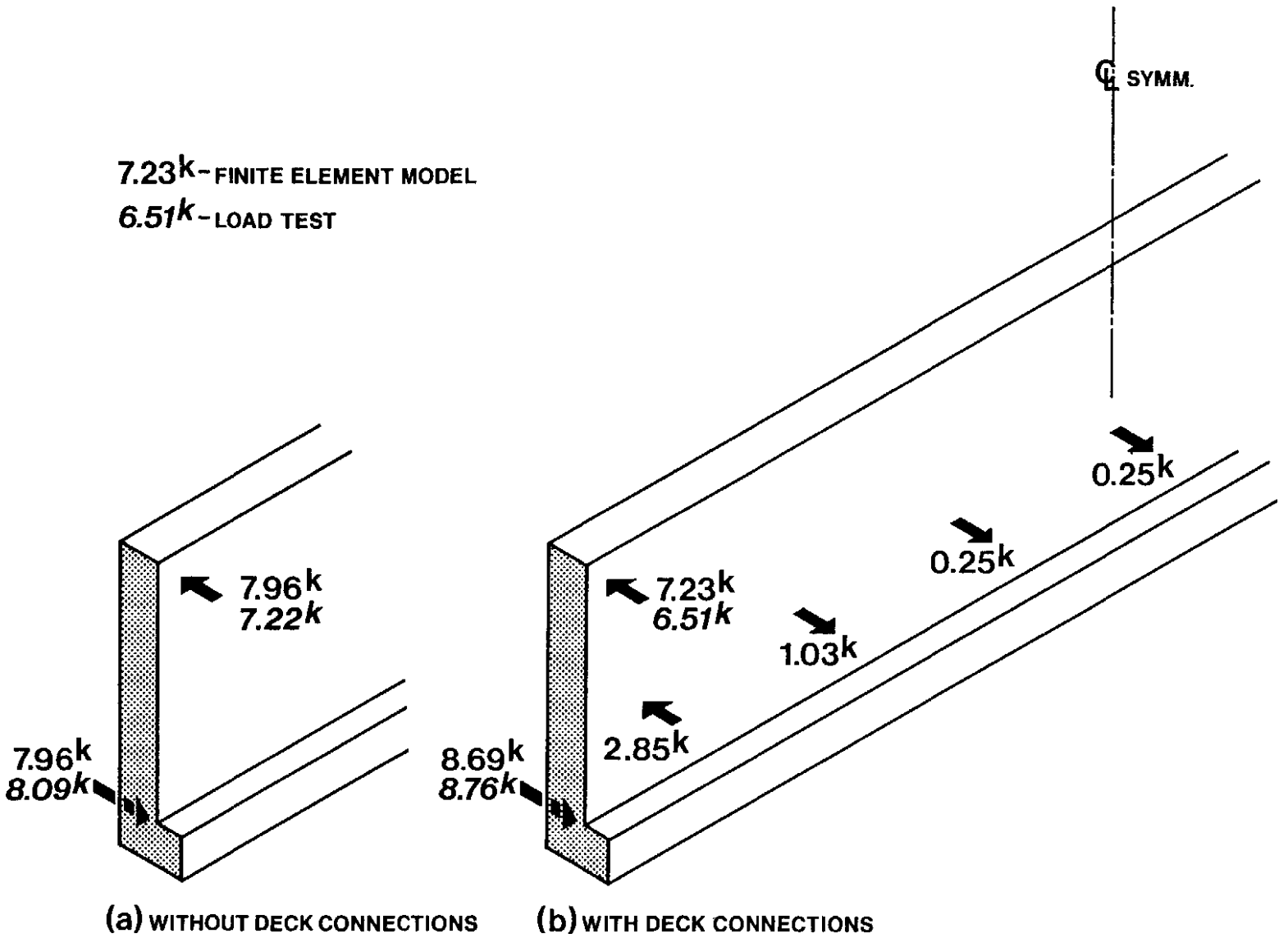

Fig. 3.3 - Horizontal forces acting on L-beam

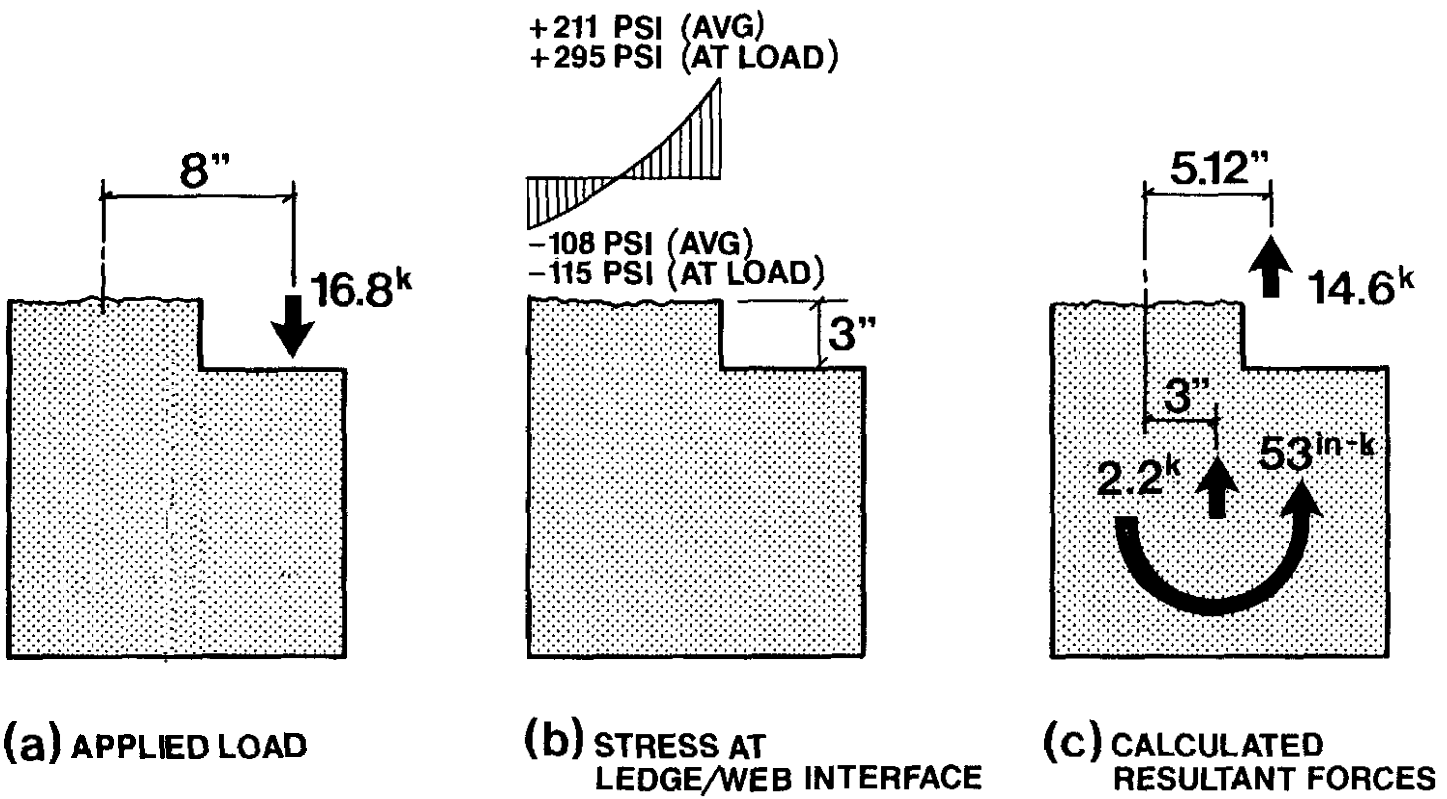

Fig. 3.4 - Study of ledge region from finite element model

4. LOAD TESTS

Two L-beams and one pocket spandrel were tested to study their behavior and verify their strength. The tests were conducted in the structural laboratory of Wiss, Janney, Elstner Associates in Northbrook, Illinois.

4.1 Test Specimens

General. All three spandrels were 72 in. high, 8 in. wide and 2.8 ft long. The target design loads were based on 90 psf dead load and 50 psf live load. which are typical for a double tee parking structure with 60 ft spans. The reactions at each stem of a" 8 ft wide double tee was 16.8 kips.

Design. The design of the test specimens was based on the state-of-the-art methods described in the background section. Shear and torsion design for the prestressed spandrels followed the procedure recommended by Zia and Hsu. ACI Equation 11-10 (rather than Eq 11-11 or 11-13) was use to compute the basic shear strength provided by the concrete section. Flexural design followed ACI 318-83. Some reserve flexural strength was required to meet the provisions of Article 18.8.3. which requires a bending capacity equal to at least 1.2 times the cracking moment. Reinforcement for torsional equilibrium was checked by Equation 1. This reinforcement was not added to the reinforcement for internal torsion.

In view of the controversy regarding ledge-to-web attachment, alternate procedures were used for design of hanger reinforcement:

- Hanger reinforcement for Specimen 1 was designed by Equation 2, with a one-sixth reduction in the load suspended from the web based on relative ledge depth. All of the transverse reinforcement between ledge loads was considered to be effective, and hanger reinforcement was not added to shear and torsion reinforcement.
- Equation 3 was used for design of the hanger reinforcement in Specimen 2. A 7.4 percent reduction in the suspended load was taken based on a" assumed parabolic shear stress distribution. Again, all the hanger reinforcement between ledge loads was

considered effective, and it was not added to shear/torsion reinforcement.

- Hanger reinforcement for the pocket spandrel (Specimen 3) was designed by Equation 2. In addition to a U-bar at the pocket, one wire on each side of the pocket from the mesh reinforcing was considered to contribute.

Design of the dapped-end connection for the pocket spandrel basically followed the PCI Handbook procedure with two exceptions. First, due to relatively low stresses, there was no special reinforcement provided for diagonal tension in the extended end or direct shear at the junction of the dap and the main body of the member. The welded wire shear reinforcement, however, was continued into the extended end. Second, the reinforcement for flexure and axial tension in the extended end was not continued past the potential diagonal tension crack extending to the bottom corner of the beam.

Details. The dimensions and reinforcement details of the test specimens are provided in Figs. 4.1 and 4.2. The following features of the reinforcing details should be noted:

- Due to the different design methods, Specimen 2 has twice as much hanger reinforcement across the ledge-web interface. This reinforcement was provided by partial-height L-bars on the inside face of the spandrel between the stirrups. These bars add about 4 percent to the weight of the mild steel in the beam.
- Closed ties formed in one piece by overlapping 90 degree end hooks are used on the left half of the L-beams. Stirrups on the right side of the L-beams consist of lapped-spliced U-bars.
- The longitudinal bars in the L-beams are not hooked at the ends.
- At the right side of the L-beams, two #5 bars are welded to a bearing plate. A #5 U-bar is used on the left side of the L-beams.
- Wire mesh is used for shear reinforcement of the pocket spandrel. The mesh is not hooked around the main reinforcement at the top and bottom of the beam, although the ACI code

requirements for development of web reinforcement (Article 12.13.2.5) are satisfied.

Materials. Design of the test specimens was based on 5,000 psi concrete, 60 ksi reinforcing bars (ASTM A706), 270 ksi stress-relieved strand, and ASTM A497 mesh. Concrete cylinders and reinforcing bar samples were tested to determine actual strengths. The results are presented in Table 4.1. The yield strength of the X3 bars was much higher than expected.

4.2 Test Procedure

Setup. The test setup is shown in Fig. 4.3. The spandrels were supported on rigid L-shaped frames which provided lateral restraint at the four corners of the beam. Load was applied at seven points along the beam using specially designed double tees (and one single tee). To simulate long-term creep of elastomeric bearing pads, two 1/4 in. pads on either side of a 1/4 in. steel plate were used under the tee stems. The pads were 6 in. wide (measured along the beam) by 3 in. long. These dimensions were chosen so the load could be applied at the desired eccentricity without exceeding reasonable bearing stresses.

The test setup featured a removable connection between the spandrels and double tees. Pedestals were used to support the dapped ends of the pocket spandrel (Fig. 4.3b).

Instrumentation. Instrumentation included load cells at two of the loading points on the double tees. as well as all four horizontal reaction points. Three deflection transducers and one tiltmeter were set up at midspan to monitor horizontal and vertical deflections and rotations. Finally, single element strain gages were placed on selected reinforcing bars as per Table 4.3.

Load sequence. Initially, each spandrel was incrementally loaded to service load (16.8 kips per tee stem) without the connection between the double tees and spandrel. After unloading, this sequence was repeated with the deck connections in place. Finally, the beams were loaded to failure without the deck connections in increments of 2.5 kips per tee stem. The third specimen was tested to failure in two phases. After a failure near the end region in Phase 1, the supports were moved in 4 ft from each end. and the specimen was reloaded to failure.

4.3 Behavior and Strength of Test Specimens

Deflection and rotation. Figures 3.1 and 3.2 compare the measured deflections of the L-beam and pocket spandrel to those predicted by the finite element models. Although the measured deflections are quite small, they are two to three times the predicted deflections. About half of the vertical deflection and some of the rotation may be attributable to deformation of the bearing pads.

Figure 4.4 shows a plot of stem reaction vs. midspan torsional rotation of Specimen 2. The stiffness of the beam is significantly reduced after cracking was observed.

Service load behavior. At service load. no cracks were observed in the L-beams. However. minor cracks were observed "ear the dapped-end connection of the pocket spandrel. These cracks. which are shown in Fig. 4.5a, were all less than 10 mils (0.010 in.) in width.

Failure patterns - Specimen 1. The cracking patterns that occurred during loading to failure are shown in Fig. 4.6a. Diagonal cracks began to appear on Specimen 1 at a load of 25 kips per stem. The crack at the ledge/web junction occurred at 27.5 kips. This crack immediately opened to 20 mils and extended end to end where it connected to inclined cracks in the ledge. The ledge continued to separate from the web until the test was stopped at a ledge load of 34.6 kips per stem. At the end of the test, the crack at the ledge/web junction was over 1/8 in. wide, as show" in Fig. 4.7.

Failure patterns - Specimen 2. As shown in Fig. 4.6b, a well developed patter" of inclined and "rainbow" cracking developed on the inside face of Specimen 2. Typically, these cracks were less than 10 mils wide. Also, several 1 to 3 mil flexural cracks were observed on the outside face. The crack at the ledge/web junction was restrained by the additional hanger reinforcement, as shown in Fig. 4.8. At a load of 42.7 kips per tee-stem, punching shear failures occurred at the first and sixth tee stem from the left. Figure 4.9 shows the punching shear failures. The failure cone initiates behind the bearing pad. The failure surface is almost vertical "ear the top and inclined below the ledge reinforcing. As a result, the ledge flexural reinforcement is not very well developed across the failure plane.

Failure patterns - Specimen 3. The cracks which formed during Phase 1 of the Specimen 3 test are shown in Fig. 4.5b. Cracks near the dapped-end connection which developed at service load continued to lengthen and widen, and new inclined cracks formed. Cracks below the pockets began to form at tee stem loads of 18 to 25 kips. As the load was increased, diagonal tension cracks developed further from the support. These cracks typically initiated near midheight of the beam. At a load of 26.5 kips per tee stem. a diagonal tension crack near the right support extended down to the bottom corner of the beam and failure occurred immediately, as shown in Fig. 4.10.

In Phase 2 of the Specimen 3 test, a wide "rainbow" crack formed at load of about 43 kips per tee-stem. Apparently this crack is due to a combination of diagonal tension due to shear and vertical tension due to the tee-stem loads. The ultimate failure, however, occurred when the concrete below the fifth pocket from the left punched out at 47.6 kips. The "rainbow" crack and punching failure are shown in Figs. 4.5c and 4.11.

Strength. Table 4.2 summarizes the design force. calculated strength and test force for several potential and actual failure mechanisms. The calculated strengths are based on the equations used for design. Because the hanger reinforcement for Specimens 1 and 2 was designed using different equations, the calculated strength is roughly the same even though Specimen 2 had twice as much hanger reinforcement.

The calculated strength is expressed as both a "design" strength and a "predicted" strength. The design strength is based on specified material properties, and includes the appropriate strength reduction factor. The predicted strength uses actual material properties and no strength reduction factor.

As shown in Table 4.2, the spandrel beams were tested to a load near or beyond their predicted capacity for several of the primary failure mechanisms. There were, however, several notable exceptions.

The shear failure of Specimen 3 (Phase 1) occurred at the diagonal cracking load, and the expected contribution from the shear reinforcing was not realized.

The ledge-to-web attachment strength of Specimen 1 was considerably less than predicted by Equation 3. In contrast, Specimen 2 showed no sign of a ledge-to-web attachment failure. even though the test

force was slightly above the capacity predicted by Equation 2. The strength of the hanger reinforcement below the pocket of Specimen 3 (Phase 2) was well beyond the predicted capacity. Apparently, the shear strength of the concrete below the pocket contributed.

The most surprising result was the punching shear failure at Specimen 2. Although the ledge loads were quite high, the punching shear strength was only about 60 percent of the predicted capacity.

Horizontal reactions. At service loads, the measured horizontal reactions at the supports were comparable to the reactions predicted by the finite element model, as shown in Fig. 3.3.

Figure 4.12 shows a plot of tee stem load vs. horizontal reaction forces at the left support of Specimen 2. The horizontal reactions did not continue to increase proportionally with load after cracking of the L-beams. At a ledge load of 39 kips per stem, the horizontal reactions actually began to drop off. Apparently, the torsion equilibrium reinforcement on the inside face of the spandrel was yielding and eccentric bearing helped equilibrate the eccentric ledge load due to rotation at the support.

Reinforcement strain. Table 4.3 summarizes the reinforcement strain at gaged locations. Data are provided at or "ear service load, factored load and the maximum test load.

At service load reinforcement strains are insignificant except at the dapped-end connection of the pocket spandrel, where the strain in the hanger reinforcement bar nearest the load is almost 0.1 percent. This strain level corresponds to half the yield stress for a Grade 60 bar. Even though the strain levels in the ledge flexure and hanger reinforcing are very low, they are noticeably higher at the ledge load.

At factored load, cracking of the ledge/web junction of Specimen 1 was accompanied by very high hanger reinforcement strain. In Specimen 2, this cracking was limited to the vicinity of the ledge load which is reflected in the recorded strains. Strain in the ledge flexure reinforcement remains low at factored loads because there are no vertical cracks at the ledge/web junction. I" spite of early cracking at the dapped-end connection. strain levels at factored loads are well below yield strain.

At the maximum test load, the strain in the ledge hanger bars in Specimen 1 are well into the strain hardening range. The ledge hanger bars in Specimen 2 are approaching the yield strain. (Using the 0.2 percent

offset method, the yield strain of the #3 bars is about 0.5 percent.) The hanger reinforcing bars at the pocket in Specimen 3 are also near the yield strain. It should be noted that these strains would exceed the nominal yield strain of a Grade 60 bar. Strain in the ledge flexure reinforcement remains low at maximum test load, indicating the absence of ledge flexure cracks.

TABLE 4.1 – MATERIAL STRENGTHS

Concrete		Reinforcing		
Specimen	Compressive Strength f'_c (a)	Bar Size	Yield Strength f_Y (ksi)	Tensile Strength f_u (ksi)
1	5,330	#3	78.9	98.7
2	5,640	#4	70.4	103.7
3	6,060	#6	64.2	98.1

(a) Average of 3 field-cured cylinders tested concurrently with load test (psi)

TABLE 4.2 – SPANDREL DESIGN AND TEST RESULTS

Failure Mechanism	Units	Specimen No. (a)	Design Force		ø	Calculated Strength		Test Force(d)
			Service	Ultimate		Design (b) (ø x Nominal)	Predicted (c) ø = 1	
Mid-span flexure	in-kips	1	5,490	8,190	0.9	11,900 (f)	13,730	10,520
		2	5,490	8,190	0.9	11,900 (f)	13,730	12,800
		3-1	5,410	8,080	0.9	9,400 (f)	10,440	8,150
Shear at support Torsion at support	kips in-kips	1	68.0 470	101.4 709	0.85	111.1 793	145.2 1033	130.3 967
		2	68.0 470	101.4 709	0.85	111.1 793	146.8 1033	158.6 1196
		3-1	66.9 118	100.0 177	0.85	124.7 (e)	159.0 (e)	100.9 186
		3-2	66.9 118	100.0 177	0.85	124.7 (e)	159.0 (e)	124.7 238
Lateral bending due to torsion equilibrium force	in-kip	1	470	709	0.90	692	902	967
		2	470	709	0.90	692	902	1196
		3-1	118	177	0.90	246	273	186
Hanger reinforcement at dapped end	kips	3-1	66.9	100.0	0.90	95.0	113.0	100.9
Hanger reinforcement for ledge load	kips per stem	1	16.8	25.3	0.90	28.4 (g)	41.5 (g)	34.6 (k)
		2	16.8	25.3	0.90	26.8 (h)	39.1 (h)	42.7
		3-2	16.8	25.3	0.90	24.1 (j)	30.8 (j)	47.6
T-stem bearing (l)	kips per stem	1	16.8	25.3	0.70	66.8	101.7	34.6
		2	16.8	25.3	0.70	66.8	107.6	42.7
		3-2	16.8	25.3	0.70	66.8	115.6	47.6
Ledge punching shear at interior bearing(m)	kips per stem	1	16.8	25.3	0.85	61.7	74.9	34.6
		2	16.8	25.3	0.85	61.7	77.1	42.7
Ledge punching shear at exterior bearing(n)	kips per stem	1	16.8	25.3	0.85	53.7	65.2	34.6
		2	16.8	25.3	0.85	53.7	67.1	42.7

(a) 3-1 and 3-2 indicate Phase 1 and 2 of the Specimen 3 load test, respectively

(b) Calculated nominal strength using state-of-the-art design equations and specified material properties (multiplied by ø).

(c) Calculated nominal strength using design equations and actual material properties (ø = 1)

(d) [ ] - indicates failure at specified test force

(e) Torsion design not required.

(f) Reserve flexural strength was required to meet the requirements of Article 18.8.3 of ACI 318-83 which requires a bending capacity equal to at least 1.2 times the cracking moment.

(g) Hanger reinforcement designed by Eq. 2 with a one-sixth reduction in the load suspended from the web based on relative ledge depth.

(h) Hanger reinforcement designed by Eq. 3 with a 7.4 percent reduction in the load suspended from the web based on parabolic shear stress distribution.

(j) Hanger reinforcement designed by Eq. 2; one wire on each side of pocket included.

(k) Hanger reinforcement yield at 29.9 kips per stem.

(l) Bearing design per PCI Eq. 6.8.1 with $N_u = 0$.

(m) Using PCI Eq. 6.14.1.

(n) Using PCI Eq. 6.14.2.

TABLE 4.3 - REINFORCEMENT STRAINS

Location	Gage No. (a)	Distance from load (in)	Service Load		Factored Load		Max Test Load	
			Load (b)	Strain (%)	Load (b)	Strain (%)	Load (b)	Strain (%)
Ledge hanger reinforcement (near midspan)	l-l	0	16.9	0.004	27.3	0.239	34.6	(c)
	l-2	12	16.9	0.001	27.4	0.120	35.6	3.211
	l-3	24	16.9	0.0	27.4	0.223	34.6	2.235
	1-4	12	16.9	0.0	27.4	0.245	34.6	(c)
	1-5	0	16.9	0.003	27.4	(c)	34.6	(c)
Ledge flexure reinforcement	l-6	24	16.9	-0.002	27.4	0.016	34.6	.015
	l-7	0	16.9	-0.001	27.4	0.026	34.6	0.042
Ledge hanger reinforcement (near midspan)	2-l	24	16.7	0.0	28.1	0.005	4i.7	(c)
	2-2	18	16.7	0.001	28.1	0.007	42.7	0.210
	2-3 (c)	12						
	2-4	6	16.7	0.002	28.1	0.023	42.7	0.412
	2-5	0	16.7	0.004	28.1	0.035	42.7	(c)
Ledge flexure reinforcement	2-6	24	16.7	-0.002	28.1	-0.003	42.7	0.016
	2-7	0	16.7	-0.001	28.1	0.007	42.7	0.034
Dapped end flexure reinf.	3-l	8	16.7	0.056	24.9	0.130	----	-----
Dapped end hanger reinf.	3-2	8	16.7	0.091	24.9	0.097	----	-----
	3-3	11	16.7	0.017	24.9	0.067	----	-----
Hanger reinf. at pocket (at midspan)	3-4	6	16.7	0.006	24.9	0.101	46.8	0.414
	3-5	6	16.7	0.005	24.9	0.093	46.8	0.162

(a) First number indicates specimen number
(b) Average ledge load (kips)
(c) Bad readings due to gage failure or bending in bar at crack

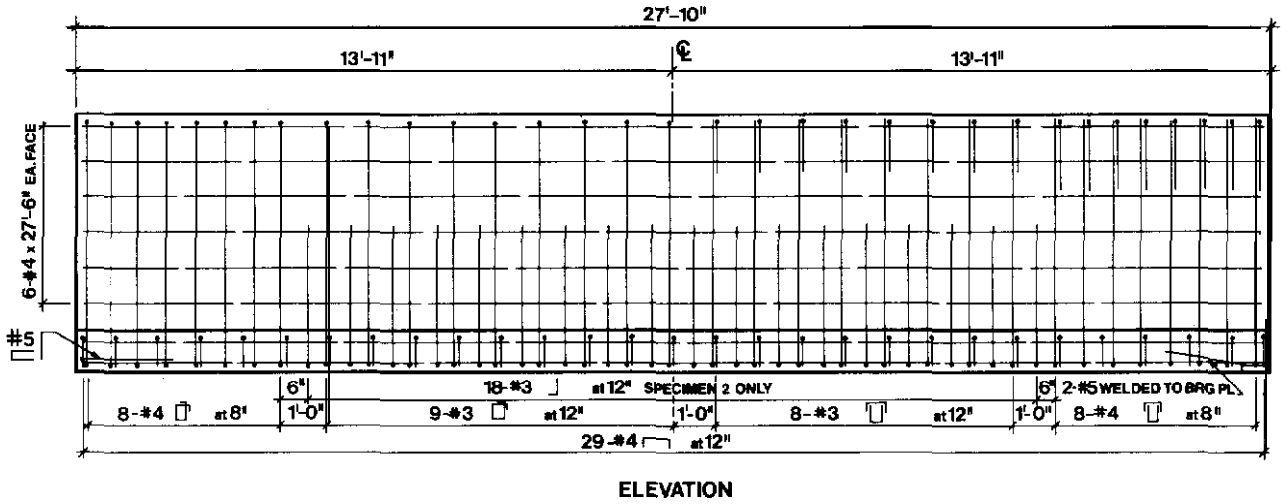

ELEVATION

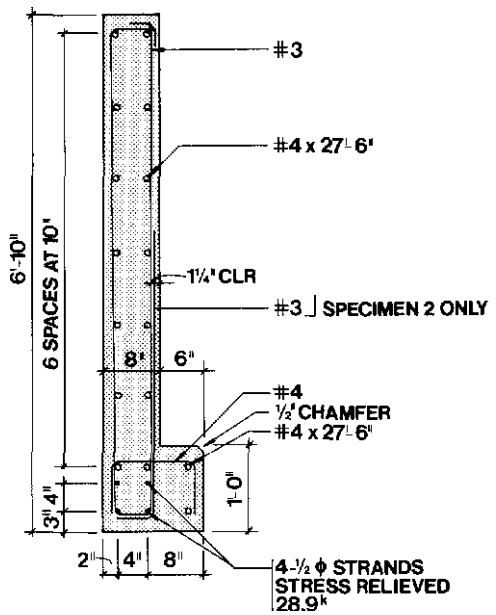

SECTION

Fig. 4.1 – Dimensions and details of Specimens 1 and 2

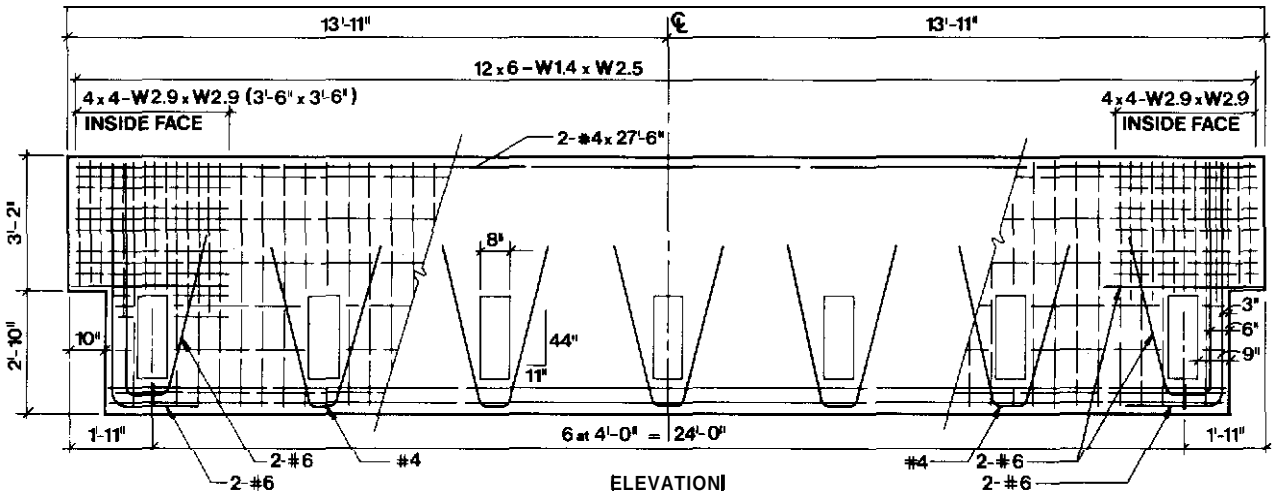

ELEVATION

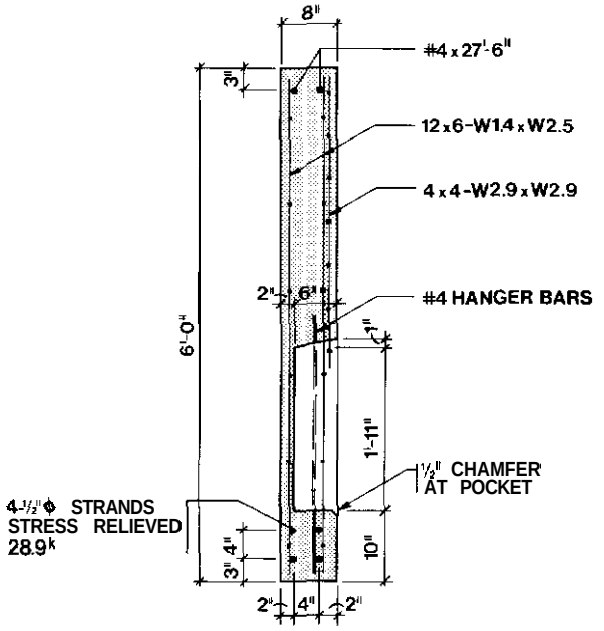

SECTION

Fig. 4.2 – Dimensions and details of Specimen 3

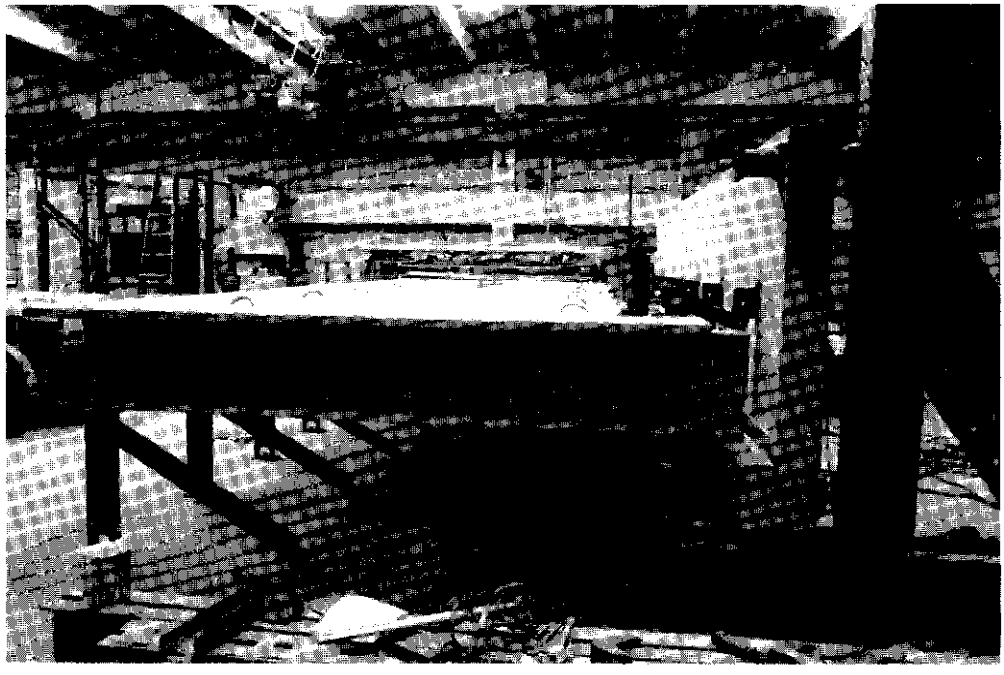

(a) L-Beams

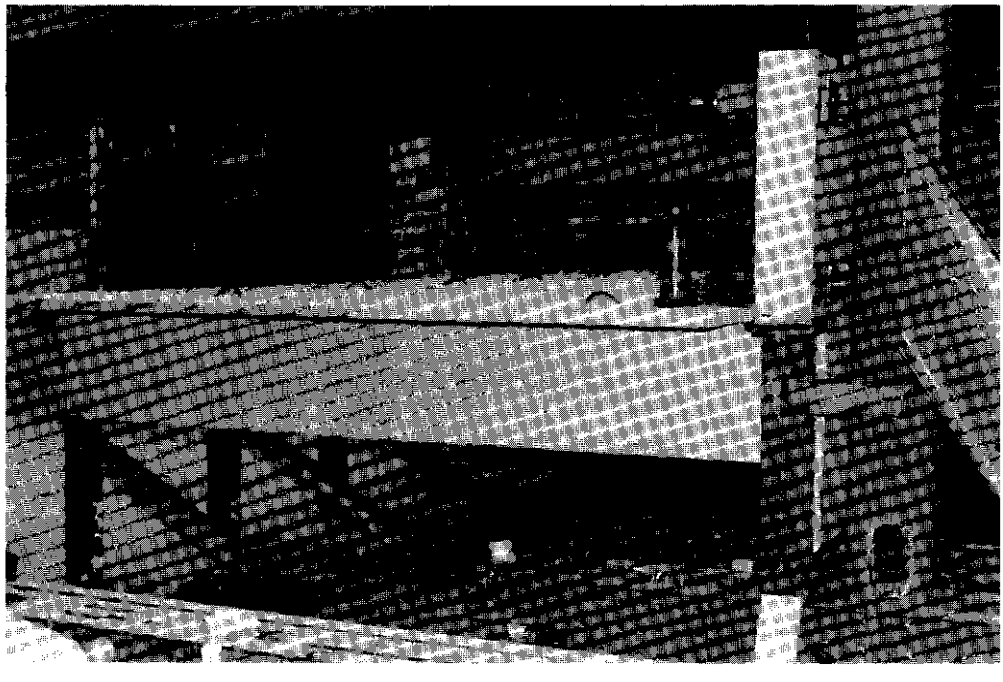

(b) Pocket spandrel

Fig. 4.3 - Test setup

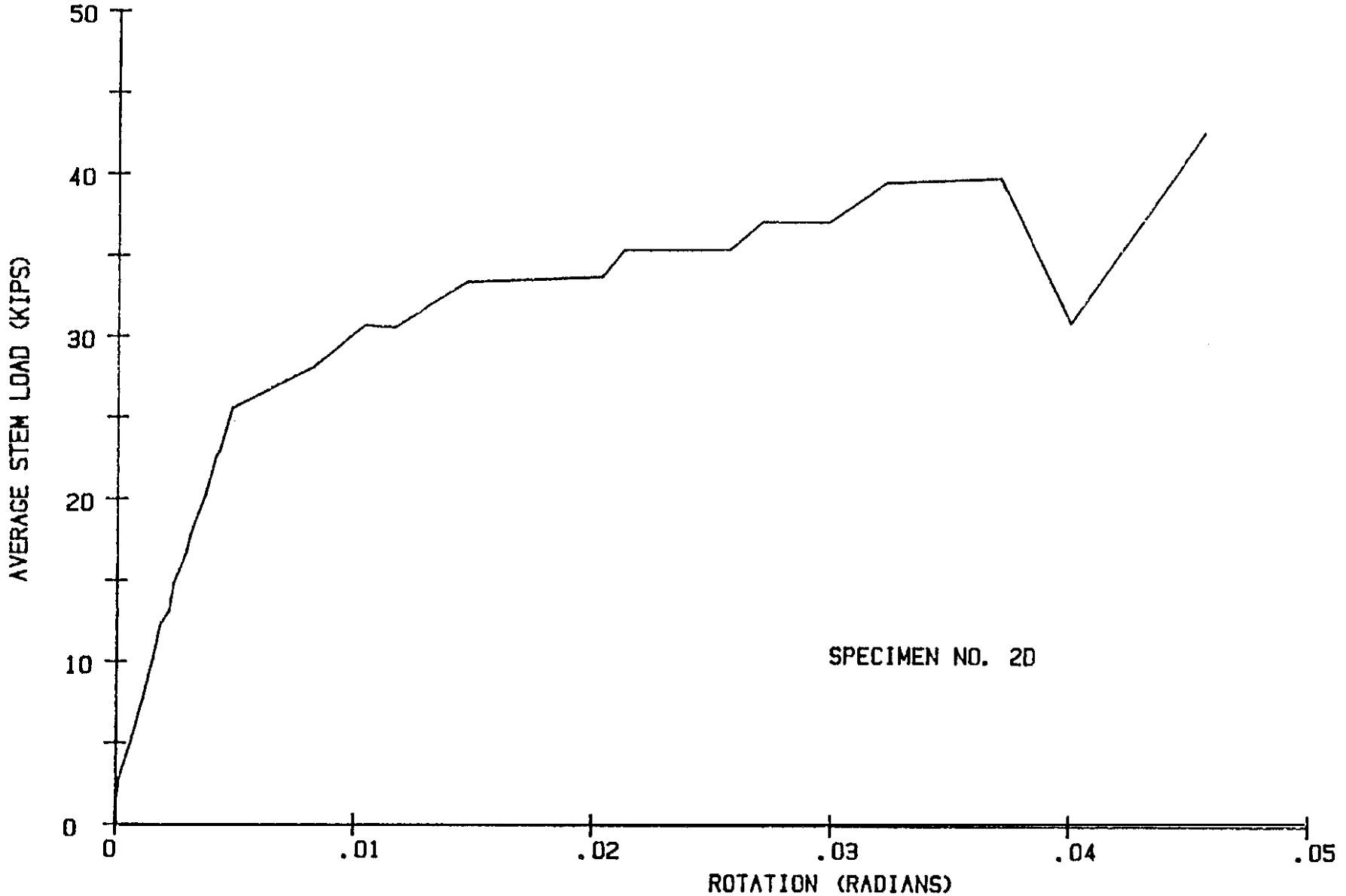

Fig. 4.4 - Stem reaction vs rotation - Specimen 2

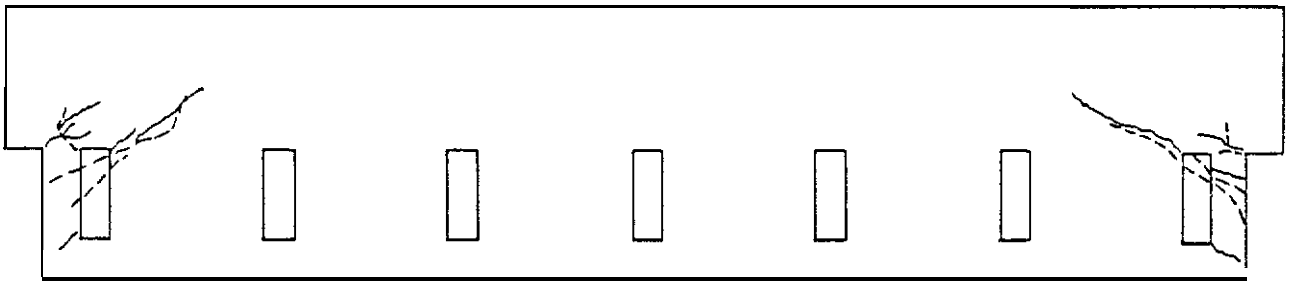

(A) FRONT ELEVATION OF SPECIMEN 3

AT SERVICE LOAD

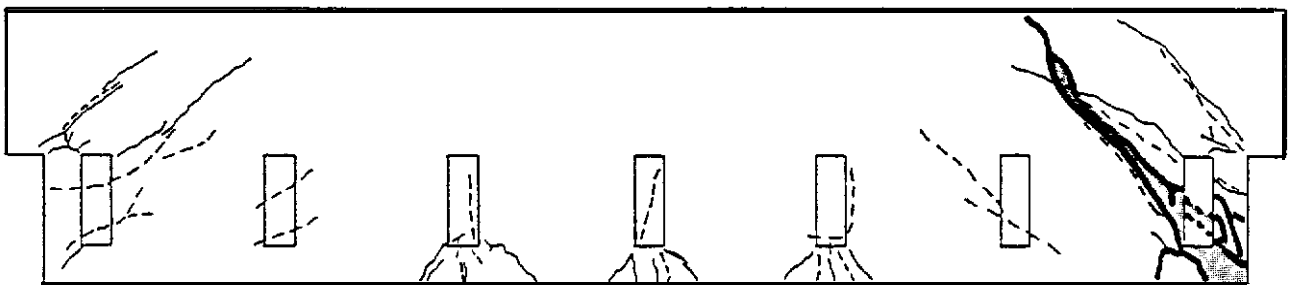

(B) FRONT ELEVATION OF SPECIMEN 3-(PHASE 1)

AT ULTIMATE LOAD

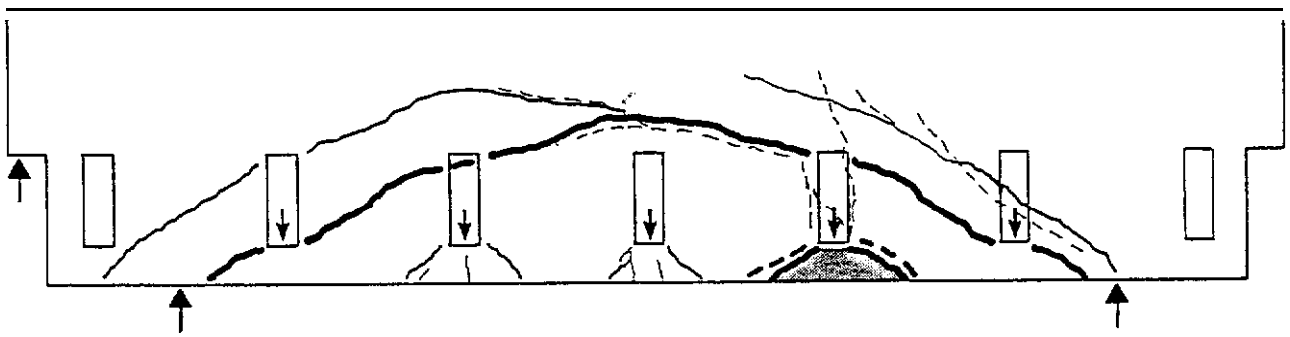

(C) FRONT ELEVATION OF SPECIMEN 3-(PHASE 2)

AT ULTIMATE LOAD (END REGION CRACKS NOT SHOWN)

CRACK LEGEND:

1-10 MIL

11-49 MIL

50 MIL OR MORE

CRACK ON BACK (OUTSIDE) FACE

Fig. 4.5 - Crack patterns - Specimen 3

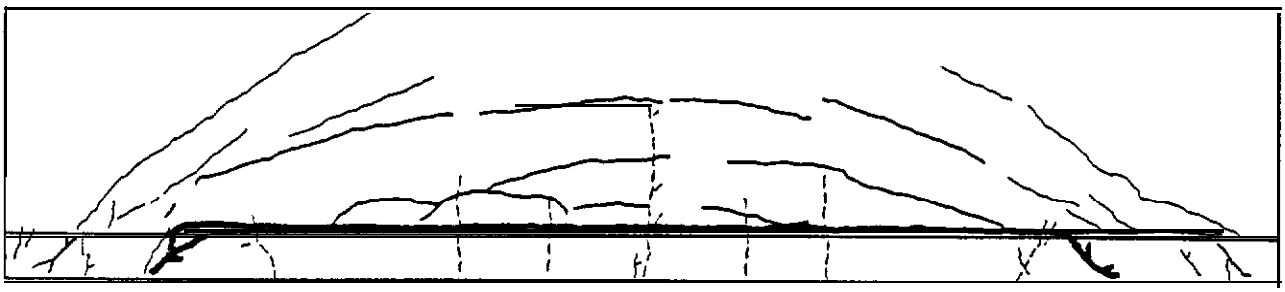

(A) FRONT ELEVATION OF SPECIMEN 1

AT ULTIMATE LOAD

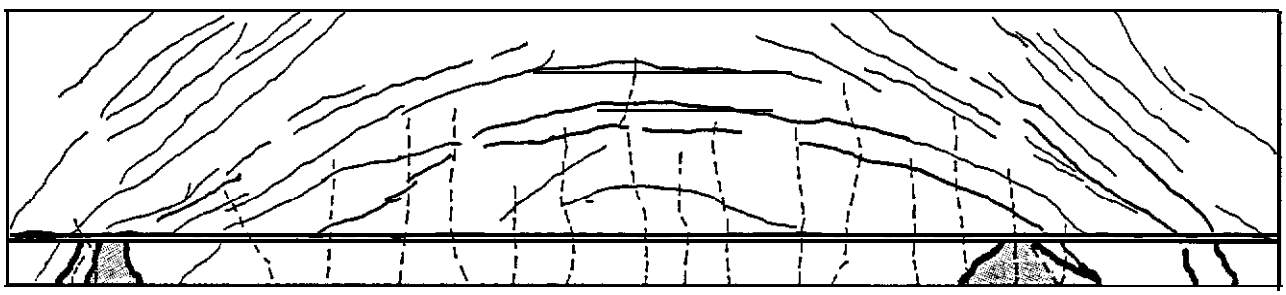

(B) FRONT ELEVATION OF SPECIMEN 2

AT ULTIMATE LOAD

CRACK LEGEND:

1-10 MIL

11-49 MIL

50 MIL OR MORE

----- CRACK ON BACK (OUTSIDE) FACE

Fig. 4.6 - Crack patterns - Specimens 1 and 2

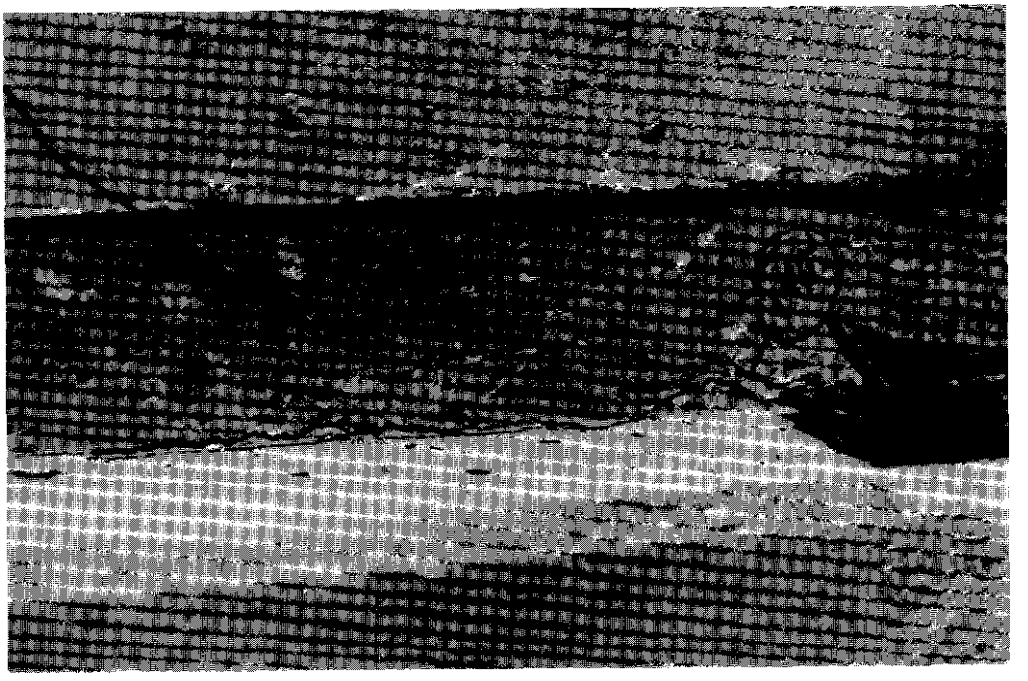

Fig.4.7 – Crack at ledge/web junction – Specimen 1

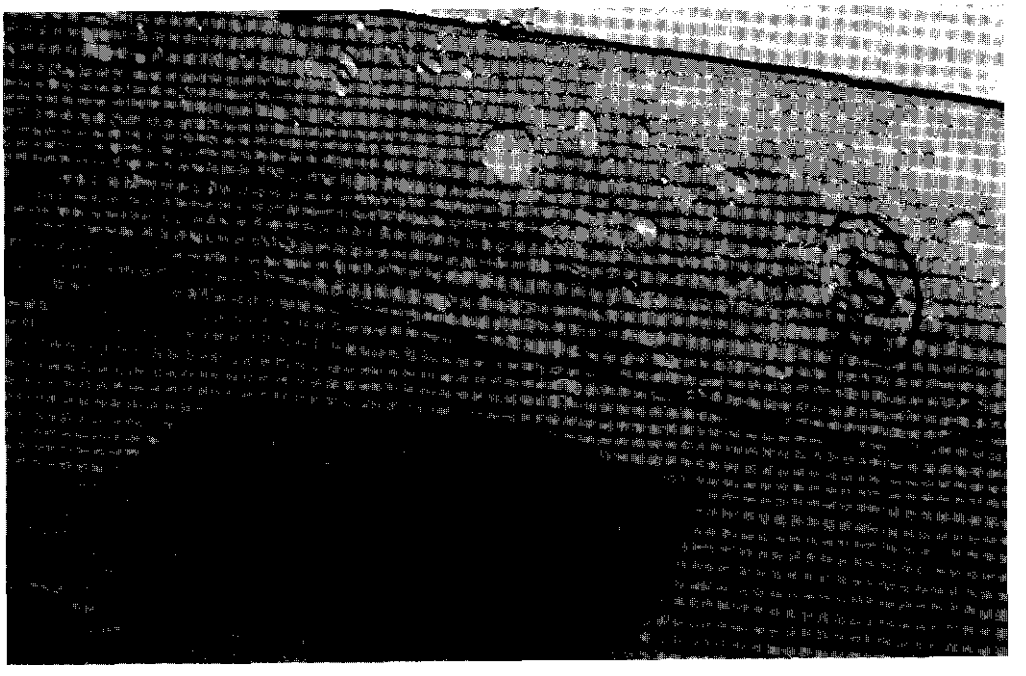

Fig.4.g – Crack at ledge/web junction – Specimen 2

(a) T-stem at left support

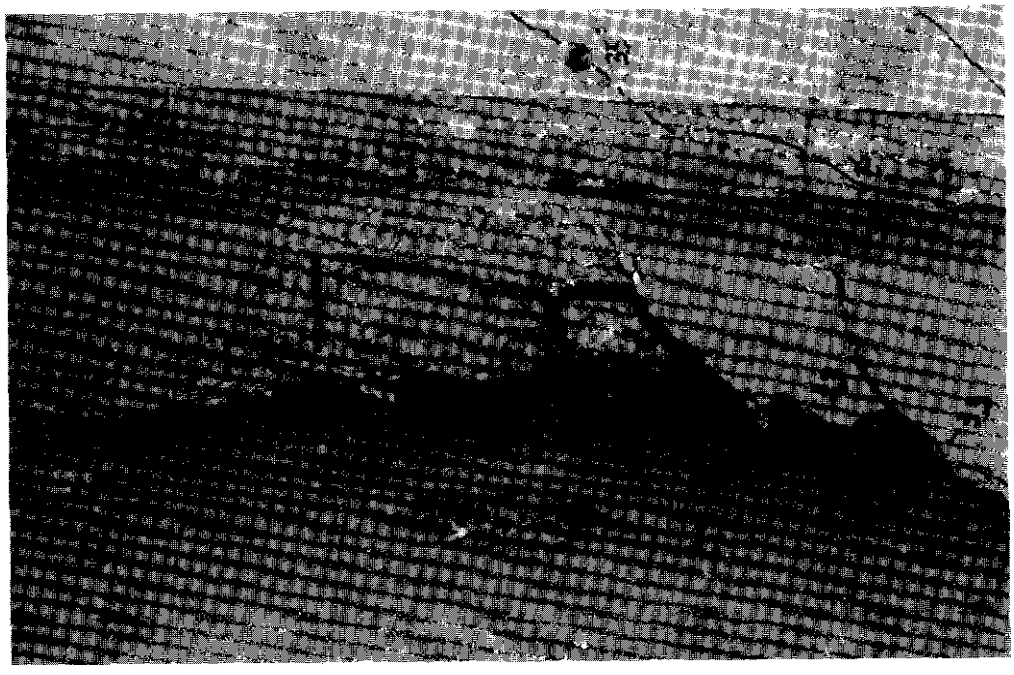

(b) 6th T-stem from left

Fig. 4.9 - Punching shear failures - Specimen 2

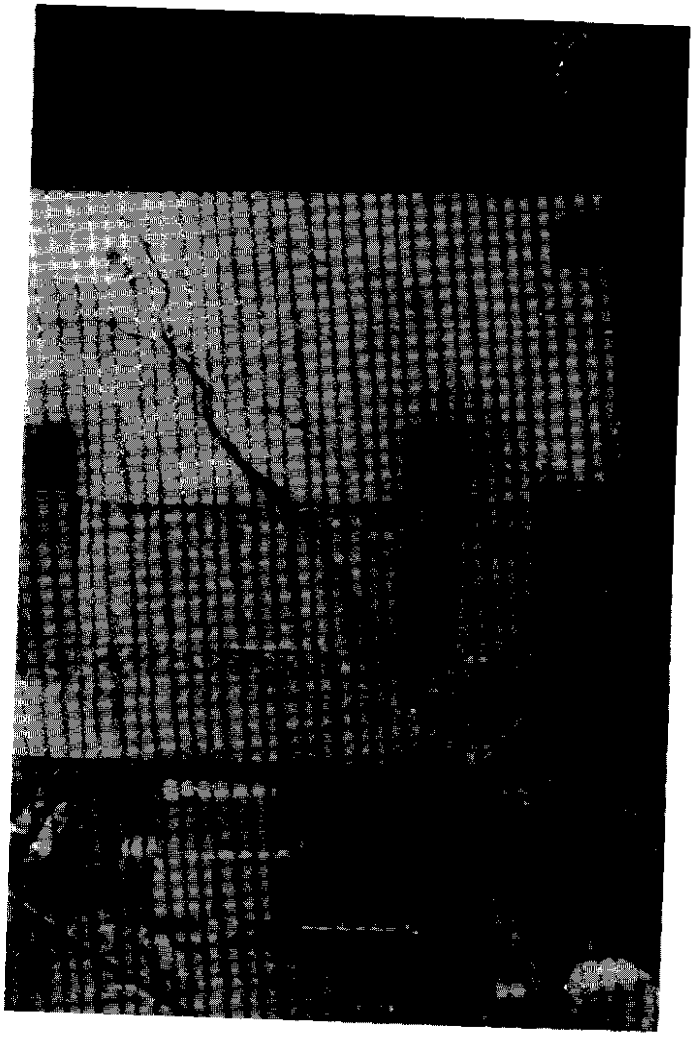

(a) front

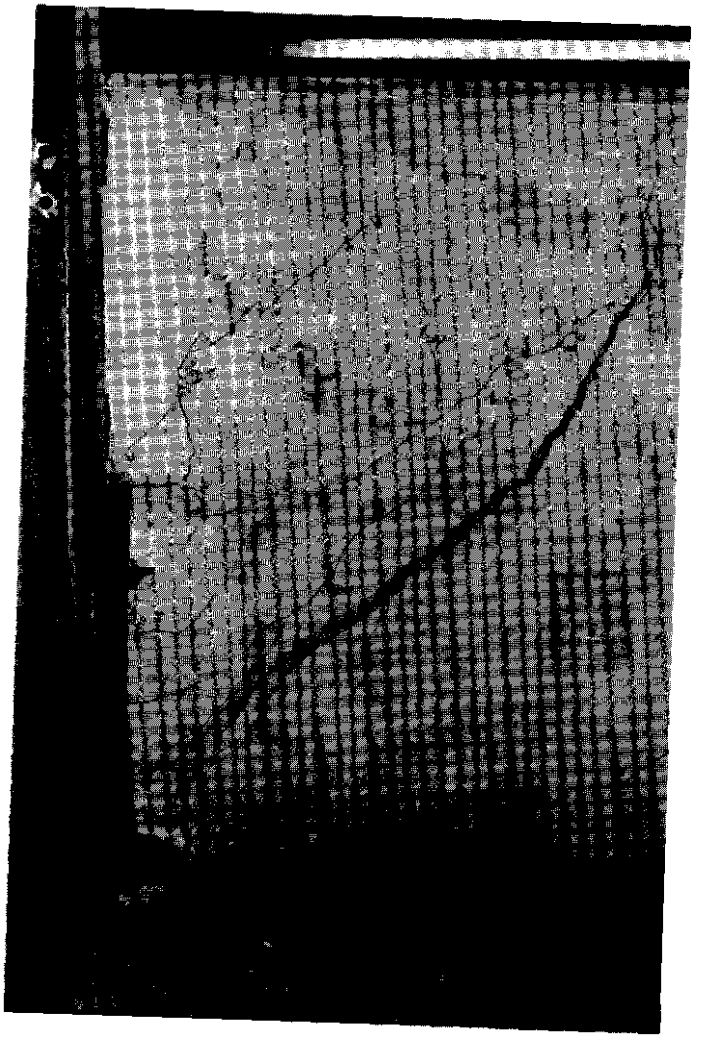

(b) back

Fig. 4.10 - Shear failure Specimen 3 Phase 1

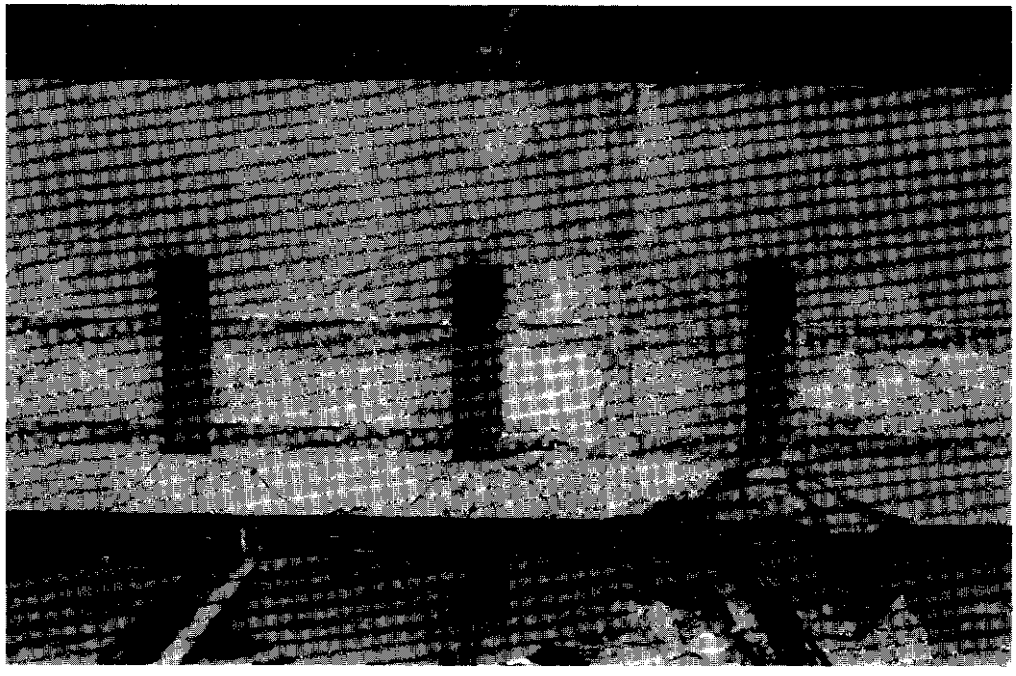

Fig. 4.11 – "Rainbow" crack and punching failure – Specimen 3 – Phase 2

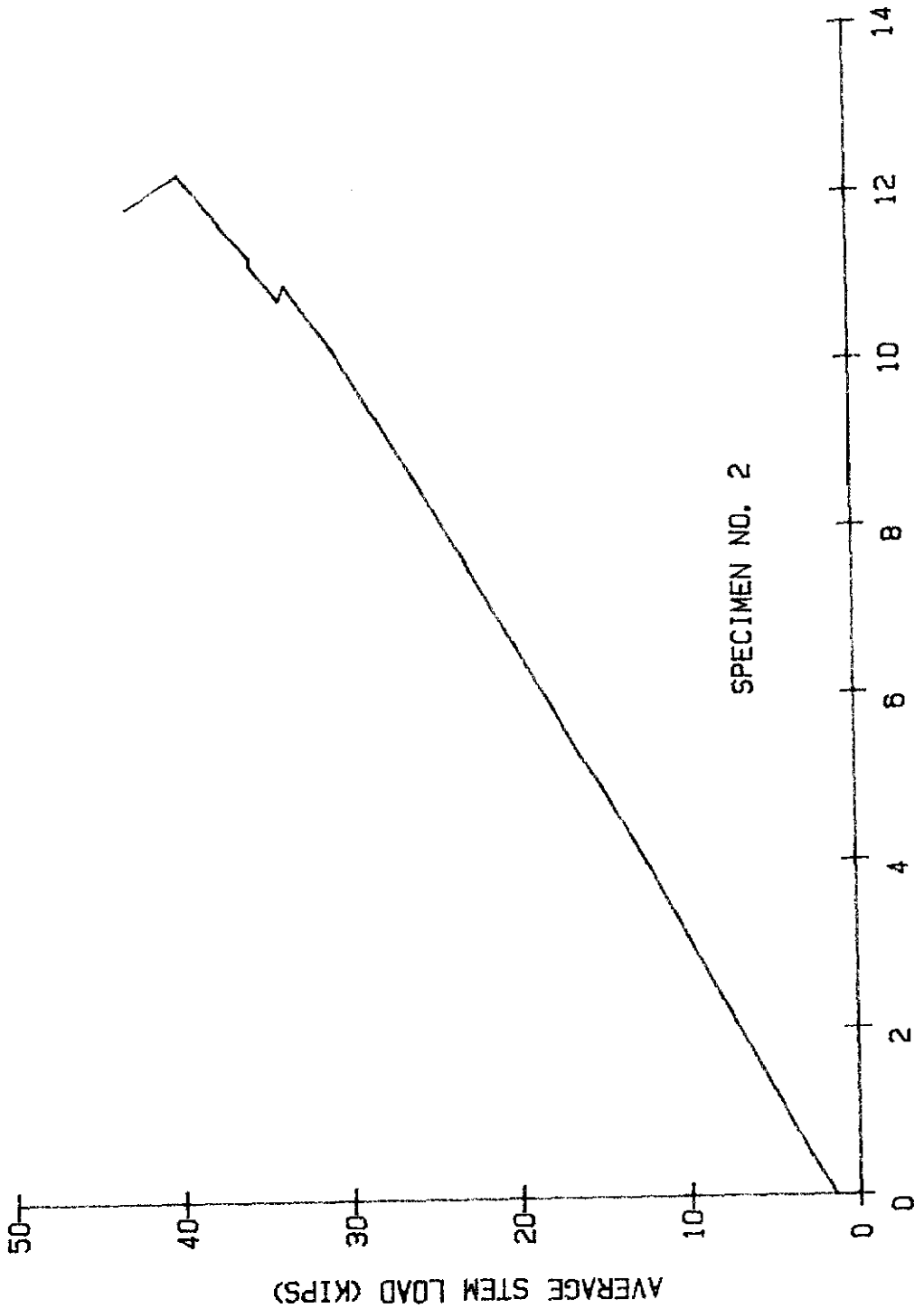

Fig. 4.12 - T-stem load vs horizontal reaction

5. ANALYSIS AND DISCUSSION

5.1 General Design Considerations

Location of critical section. The shear failure of Specimen 3, shown in Fig. 4.10. confirms the possibility of an inclined failure plane which carries all of the loads acting on the spandrel. The crack patterns which occurred in Specimens 1 and 2 suggest a similar possibility. Therefore, the shear and torsion design of spandrel beams should consider a critical section at the face of the support.

Alternately, if separate hanger reinforcement is provided to transfer the ledge loads to the top of the beam, the spandrel can be designed as a directly loaded beam with a critical section at d or h/2 from the support for non-prestressed and prestressed spandrels, respectively. However, this approach may lead to excessive transverse reinforcement in the midspan region because hanger reinforcement is added to shear and torsion reinforcement.

Influence of deck connections. As illustrated *in* Fig. 3.3, the connections to deck elements do not substantially reduce torsion. The only significant effect of the deck connections is the restraint of lateral displacement induced by bending about the weak principal axis.

5.2 Flexure

With regard to flexure, both the strength and serviceability-related behavior of the test specimens was satisfactory. It is worth mentioning, however, that flexural cracking of the L-beams only showed up on the back face. This observation is attributable to bending about the weak principal axis.

5.3 Shear and Torsion

Prestressed L-beams. Specimens 1 and 2 were tested at load levels roughly equal to the predicted capacity based on the Zia-Hsu equations. which was the basis for their design. There was no evidence that the negative bending capacity required by compression field theory was needed.

As discussed later, some level of positive bending capacity at the face of the support is required.

Pocket spandrels. The premature shear failure through the full section of the pocket spandrel near the dapped connection is attributable to poor anchorage of the primary flexural reinforcement at the bottom corner of the beam. It may have helped to extend the dapped-end flexural reinforcement beyond the inclined crack: this reinforcement, however, is not very efficient in a deep dap.

Recent research under PCIFSRAD Project #6 emphasizes the importance of anchoring the primary flexural reinforcement at dapped connections. This research concludes that the reaction should be limited to the shear strength of the web (the lesser of V_{ci} and V_{cw}) because the primary flexural reinforcement is typically not anchored at the bottom corner of the beam. The example in Appendix C illustrates a procedure for designing a dapped connection in a pocket spandrel.

Predicting the strength of the concrete section is complicated by the pockets. Hanson[16] found that a conservative prediction of the strength of concrete joists with square openings, but without stirrup reinforcement, was obtained by calculating the load at which cracking at the corner of the opening develops, assuming the shear is distributed in proportion to the area of the section above and below the opening. One approach to calculating this load is to substitute $b_w(d-h_p)$ for $b_w d$ in ACI Code equations for the shear strength of the concrete section (Equations 11-3 or 11-6 for non-prestressed spandrels, or Equations 11-10, 11-11 or 11-13 for prestressed spandrels), where h_p is the height of the pocket. Similarly, the strength provided by the shear reinforcement, V_s, is given by

$$V_s = \frac{A_v f_y (d-h_p)}{s} \qquad (4)$$

which reflects an unfavorable crack pattern through the pocket region, as shown in Fig. 5.1. The above approach is believed to be conservative for pocket spandrels. but is not generally applicable to beams with square openings. Using ACI Code Equation 11-13 and substituting $b_w(d-h_p)$ for $b_w d$, the predicted shear strength provided by the concrete section of Specimen 3

is 110 kips or 93 kips, depending on whether or not the prestress is considered to contribute to shear strength. These predictions are comparable to the failure load of 101 kips.

It is common practice not to use a deep pocket for the T-stem nearest the support. A welded bracket or Cazaly hanger is used instead. In these cases, the h_p term need not be included for design of the end region.

Detailing practices. The torsional response of deep spandrels is dominated by out-of-plane bending. There was no evidence of spalling of the side cover which can occur in compact sections subjected primarily to torsion. The use of lapped-splice stirrups in lieu of closed stirrups did not appear to have any detrimental effect, and the absence of hooks on the longitudinal reinforcement did not lead to any apparent problems.

It is unlikely that there would have been any improvement in shear strength of the pocket spandrel had the wire mesh been anchored by a bend at the longitudinal reinforcement. The failure is attributable to poor anchorage of the primary flexural reinforcement, and there was no sign of an anchorage failure of the wire fabric.

5.4 Beam End Design

Torsion equilibrium reinforcement. The applied torsional load on Specimens 1 and 2 was beyond the predicted capacity of the torsion equilibrium reinforcement required by Equation 1. To some extent eccentric bearing may have helped equilibrate the applied torsional load. Nonetheless, the test results support the contention that reinforcement for the torsion equilibrium reaction need not be added to the reinforcement for internal torsion.

Longitudinal reinforcement at end. The premature failure near the dapped connection points out a possible deficiency at non-dapped spandrel beam supports. Figure 5.2 shows the forces acting on a free body cut off by diagonal tension cracks at the support. Neglecting the distance from the top of the beam to the compressive force. the developed force required at the face of the support is given by

$$\phi A_s f_{sd} = N_u h/d + V_u (0.5+a/d) \qquad (5)$$

where f_{sd} = developed stress in the reinforcement at the face of the support. The remaining notation is defined in Fig. 5.2. For a dapped spandrel, a similar check of the free body forces across an inclined crack through the full section is recommended. Typical cases are included in the design examples in Appendices B and C.

5.5 Beam Ledges

Hanger reinforcement. The load tests and analytical studies indicate that the eccentricity of the ledge load cannot be neglected in the design of hanger reinforcement. Nonetheless, not all of the load acting on the ledge is suspended from the web, and the effective eccentricity of the ledge load is significantly reduced due to torsion within the ledge. Design by Equation 2 may be somewhat unconservative, while use of Equation 3 may be overly conservative. A design procedure for hanger reinforcement has been developed based on the transverse forces acting on the free body shown in Fig. 5.3. Summation of moments about the outside face of the spandrel gives

$$A_{sh} = \frac{V_u(d+a) - \Delta V_\ell b_\ell/2 - \Delta T_\ell}{\phi f_y d} \qquad (6)$$

where ΔV_ℓ = shear in ledge (Eq. 7),

ΔT_ℓ = torsion in ledge (Eq. 8),

b_ℓ = width of the ledge measured along the bottom of the beam, and

ϕ = strength reduction factor = 0.85,

Most of the notation used for hanger reinforcement design is graphically defined in Fig. 5.4. Similar to Equation 1, the use of $\phi = 0.85$ instead of 0.9 compensates for the ratio of internal moment arm to total effective depth.

The finite element model study verified that the shear in the ledge, ΔV_ℓ, depends on the internal shear stress distribution, which is calculated by integrating VQ/I from the top of the ledge to the bottom of the beam. In lieu of an exact solution, the following expression, based on the parabolic shear stress distribution in a rectangular beam, gives a conservative approximation of ΔV_ℓ:

$$AV_s = V_u(3-2h_\ell/h)(h_\ell/h)^2 \quad (7)$$

where h = overall height of the beam. and

h_ℓ = height of the ledge.

ΔT_ℓ depends on the torsional stiffness of the ledge compared to the total torsional stiffness of the beam. Accordingly

$$\Delta T_\ell = V_u\, e\, \gamma_t \frac{(x^2y)_{ledge}}{\Sigma x^2 y} \quad (8)$$

where e = distance between the applied load and the centerline of the web,

$(x^2y)_{ledge} = b_\ell h_\ell^2$ or $b_\ell^2 h_\ell$, whichever is smaller,

x = shorter overall dimension of a rectangular part of a cross section, and

y = longer overall dimension of a rectangular part of a cross section.

The use of γ_t in Equation 8 is intended to avoid assigning too much torsion to the ledge. If closed stirrups are provided in the ledge γ_t = 1.0; otherwise

$$\gamma_t = \frac{T_c}{T_u} \leq 1 \quad (9)$$

where T_c = torsional moment strength provided by concrete. and

T_u = factored torsional moment at critical section.

Finally, if the end of the L-beam is dapped, the end reaction will not equilibrate V_ℓ and T_ℓ . Therefore, for dapped-end beams, the total hanger reinforcement is given by

$$\Sigma A_{sh} = \frac{\Sigma V_u (d+a)}{\phi f_y d} \qquad (10)$$

For the L-beams included in this study, Equation 6 would require about 30 to 60 percent more hanger reinforcement than Equation 2, depending on Y_t. As previously noted, the use of Equation 3 doubles the hanger reinforcements requirements compared to Equation 2. Hanger reinforcement is not additive to shear and torsion reinforcement.

The background research revealed that at least four load tests of spandrel beams were conducted by precast producers several years ago. During two of these load tests, the ledge of an L-beam separated from the web. Data pertaining to hanger reinforcement design in these two test specimens are summarized in Table 5.1. Similar to the test of Specimen 1. in these prior load tests a wide horizontal crack developed at the ledge/web junction. In each case, the test was stopped before the ledge actually fell off. All three tests indicated the ledge-to-web connection was very ductile in spite of very light hanger reinforcement. The behavior of these test specimens suggests that due to strain hardening, forces in the hanger reinforcing approaching the ultimate tensile strength can be developed. It should also be noted that as the ledge begins to rotate due to separation from the web, the ledge load shifts in towards the face of the web.

As shown in Table 5.1, the yield and ultimate ledge loads were calculated using Equation 6. The maximum test loads are comparable to the calculated ultimate load. During the 1974 test, a localized separation between the ledge and web occurred in the midspan region where ledge loads were much heavier than average (See Fig. 5.6). Therefore, the strength contribution due to shear and torsion in the ledge was significantly greater than predicted by Equation 6.

The reinforcement ratio (A_{sh}/sd, where s is the ledge load spacing) of these spandrels was roughly $100/f_y$. This amount is similar to the minimum requirement for structural slabs. In view of the ductility

demonstrated in these tests, a minimum reinforcement ratio of $100/f_y$ is recommended for hanger reinforcement. The effective distribution width for hanger reinforcement is discussed later.

Ledge punching shear. The most unexpected result of the load tests was the early punching shear failures in the ledge of Specimen 2. As discussed in the background section, other researchers have found that the PCI equations for ledge punching shear may be ""conservative. One reason may be that the PCI equations do not fully account for the eccentricity between the applied load and the centroid of the critical section. This eccentricity is shown in Fig. 5.5. The analysis approach used to investigate transfer of unbalanced moment between slabs and columns can be adapted to punching shear of beam ledges. The shear stress at the inside edge of the ledge is given by

$$v_c = \frac{V_u}{b_o h_\ell} + \frac{V_u e_\ell c}{J_c} < 4\sqrt{f'_c} \qquad (11)$$

where b_o = perimeter of the critical section,

e_ℓ = distance between the ledge load and the centroid of the critical section,

c = distance between the centroid of the critical section and the inside face of the ledge, and

J_c = property of critical section analogous to polar moment of inertia (See Ref. 17).

This formula assumes that the full height of the ledge is effective and none of the eccentricity is resisted by ledge flexure. The computed punching shear capacity of Specimen 2 using Equation 11 is 40.5 kips. which is comparable to the failure load of 42.7 kips. Punching shear capacity can be improved by increasing the ledge projection or depth. The use of developed ledge flexure reinforcement should also increase punching shear capacity.

Equation 11 can not be accurately applied to conditions where flexural reinforcement developed across the critical section can help resist eccentricity. Also, shear and tensile stresses acting on the full section may reduce the punching shear resistance of the ledge. However, this study provides evidence that the PCI design equations may be unconservative in some situations, and further research is recommended.

Distribution of ledge reinforcing. In the L-beam specimens showed evidence of higher stresses in the ledge hanger and flexure reinforcement in the vicinity of the applied load. The finite element model showed a similar concentration of stress. However, the hanger reinforcement strain was much more evenly distributed after the horizontal crack at the ledge/web junction had fully developed. As the ledge separated from the web along the entire length of Specimen 1, it was clear that all of the hanger reinforcement between ledge loads was effective. Ledge flexural cracks did not develop, so nothing was learned about the post-cracking distribution of strain in ledge flexure reinforcement.

Of course. these results are only applicable to L-beams with geometry and reinforcement similar to the test specimens. Local ledge failures are conceivable, particularly if the loads or load spacing are not uniform. Figure 5.6 shows two local failures in which the ledge flexure or hanger reinforcement assumed to resist each ledge load is not fully effective. However, the shear and torsional strength across the inclined failure planes abc and def contribute to the strength. This contribution is related to the punching shear strength of the ledge. Even though the ledge reinforcing and shear strength may not be fully additive, premature failures of the type shown in Fig. 5.6 are unlikely. On the other hand, if reinforcement at the ledge load is required to supplement the punching shear strength, the ledge flexural reinforcement and hanger reinforcement should also be concentrated at the ledge load.

Figure 5.7 shows a local separation between the ledge and web related to the bending strength of the ledge. Assuming the hanger reinforcement stress is evenly distributed between ledge loads (and neglecting ΔV_ℓ) the upward force between loads is equal to V_u/s, where Vu is

the stem reaction and s is the ledge load spacing. The corresponding sum of the negative and positive bending moments in the ledge is equal to $V_u s/8$. The reinforcement required to resist this bending moment is given by

$$A_{s\ell} = \frac{V_u s}{8\phi d_\ell f_y} \qquad (12)$$

where $A_{s\ell}$ = ledge reinforcement in the top or bottom of the ledge in addition to reinforcing required for the primary moment,

d_ℓ = effective depth of $A_{s\ell}$, and

ϕ = strength reduction factor = 0.85.

Once again. use of a strength reduction factor equal to 0.85 instead of 0.9 compensates for the ratio of internal moment arm to total effective depth.

In summary, this research suggests that all of the hanger reinforcement or ledge flexure reinforcement between ledge loads can be considered effective providing the punching shear and longitudinal bending strength (Eq 12) of the ledge are adequate. Further testing should be carried out to verify this assertion.

5.6 Beam Pockets

During Phase 2 of the Specimen 3 test, the concrete below one of the beam pockets punched out at a load of 47.6 kips. The predicted failure load based on yielding of the hanger reinforcement is 30.8 kips. The difference is apparently due to a punching shear strength contribution. Based on Equation 11. the predicted punching shear strength is 31.1 kips per stem. Fully developed inclined cracks below the pocket were observed at tee stem loads of 25 kips. These results indicate that the strength contributions from hanger reinforcement and punching shear are not fully additive.

TABLE 5.1 - LOAD TESTS OF L-BEAMS WHICH FAILED DUE TO LEDGE SEPARATION FROM WEB[a]

Load Test	Spandrel Dimensions (in.)						Hanger Reinforcement					γ_t	Calc. Ledge Load (b)		Max. Test Load
	h	h_1	b_w	b_1	d	a	Amount	Grade	f_y	E	f_u		At Yield	Ult.	(kips)
PCI 9/85 Specimen 1	72	12	a	14	6.5	5.5	# 3 @ 12" (0.44 $in.^2$)	60	78.9[c]		98.7[c]	0.62	23.1	29.0	34.6
												1.0	25.9	32.4	
Thomas Conc. Prod. 1/80	80	11-3/4	6	12	3.75	4.25	# 4 @ 18" (0.53 $in.^2$)	40	55[d]		80[d]	1.0	20.9	30.4	29.2
Concrete Masonry Corp. 9/74	72	12	8	16	6.5	5.5	# 4 @ 24"[e] (0.45 $in.^2$)	60	70[d]		100[d]	0.59	21.3	30.4	39.2[f]
												1.0	24.4	34.9	

(a) Wide horizontal crack developed at the ledge/web junction in all three cases
(b) Using Eq. 6 (kips)
(c) Measured (ksi)
(d) Estimated (ksi)
(e) 4.5 ft avg. spacing of tee stems
(f) A localized separation between the ledge and web occurred in midspan region where ledge loads were much heavier than average. Therefore. the strength contribution due to shear and torsion in the ledge was significantly greater than predicted by Eq. 6.

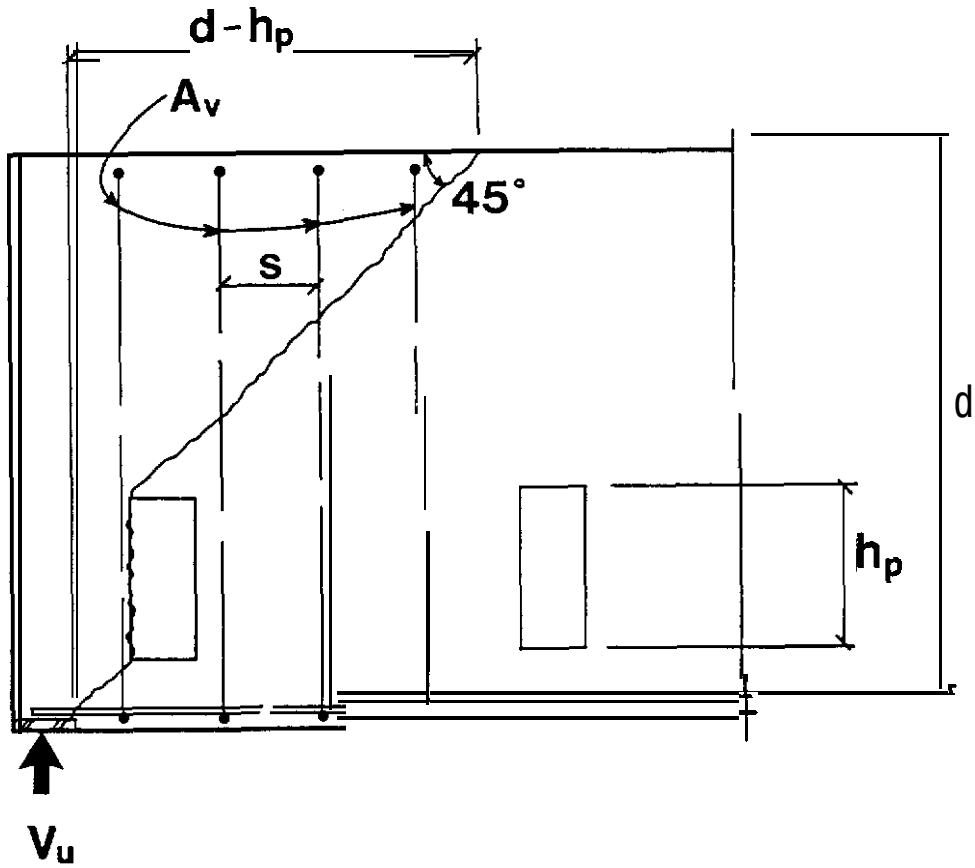

Fig. 5.1 – Shear in pocket spandrels

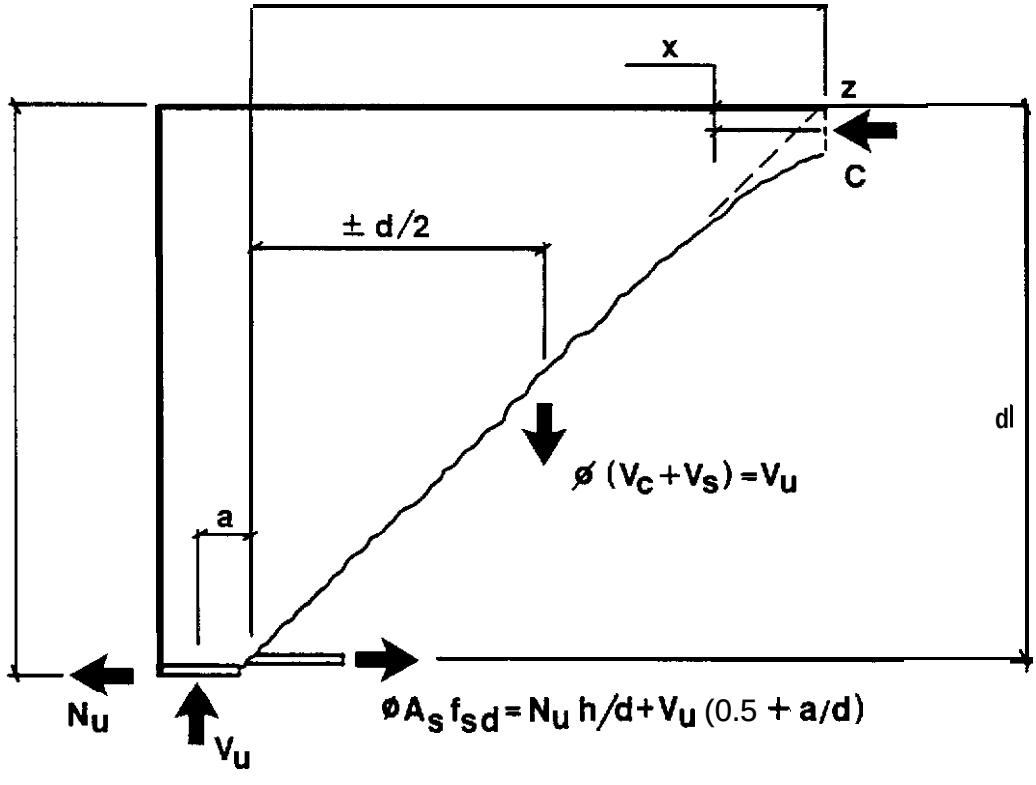

Fig. 5.2 – Forces acting on free body cut off by diagonal tension cracks at support

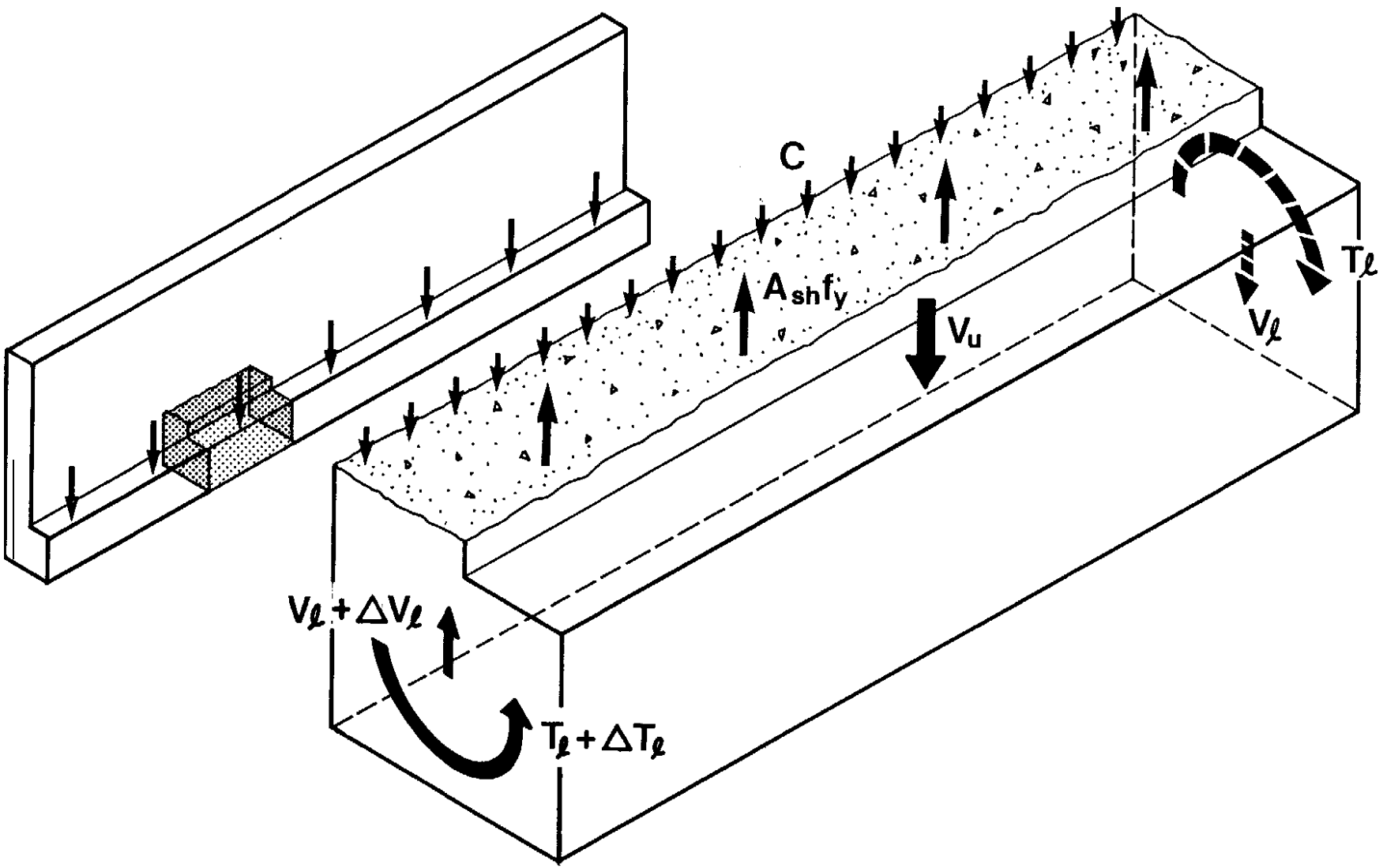

Fig. 5.3 - Transverse forces acting on free body of ledge

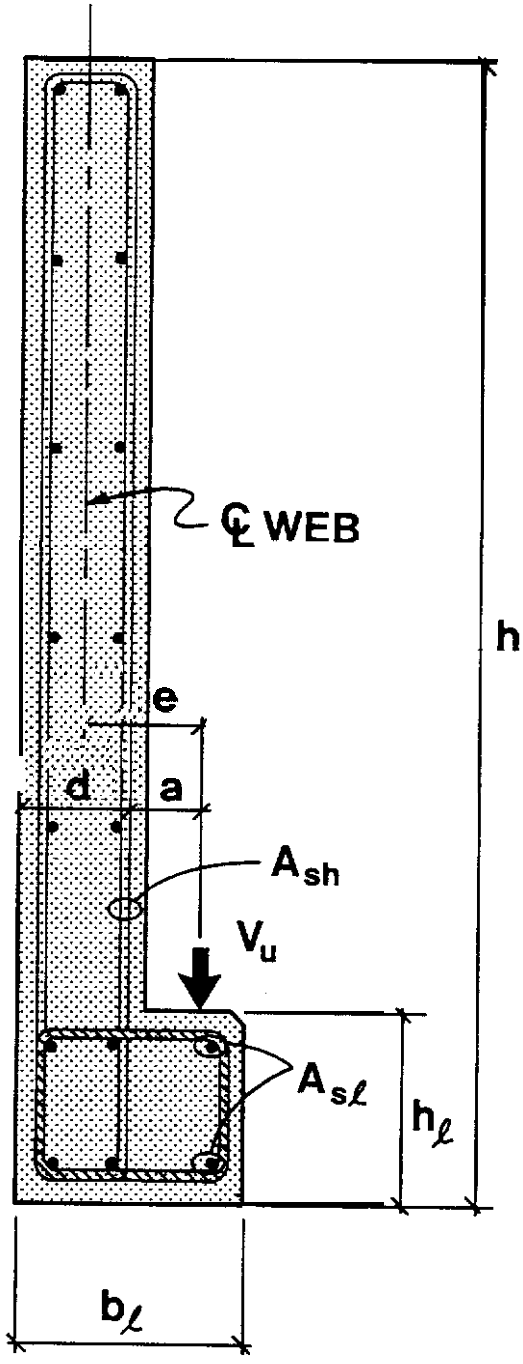

Fig. 5.4 – Notation for hanger reinforcement design

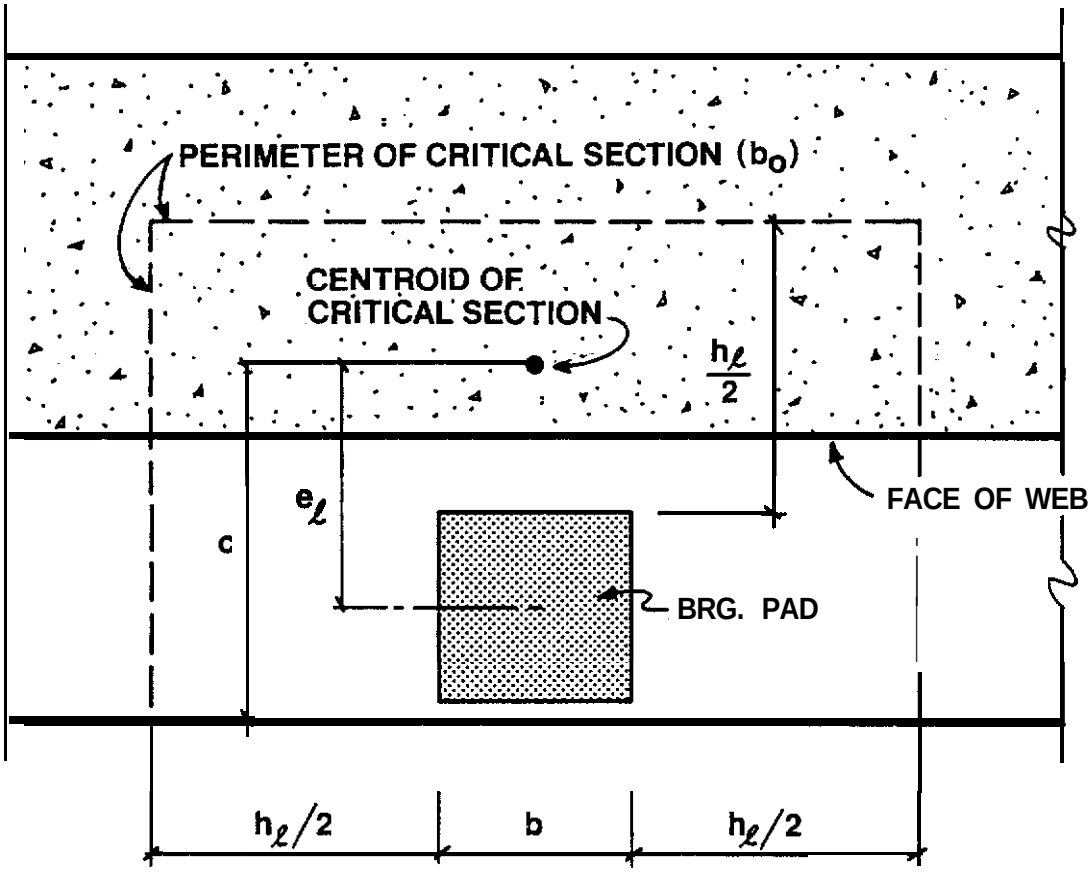

Fig. 5.5 – Plan view of ledge showing eccentricity of ledge load relative to critical section

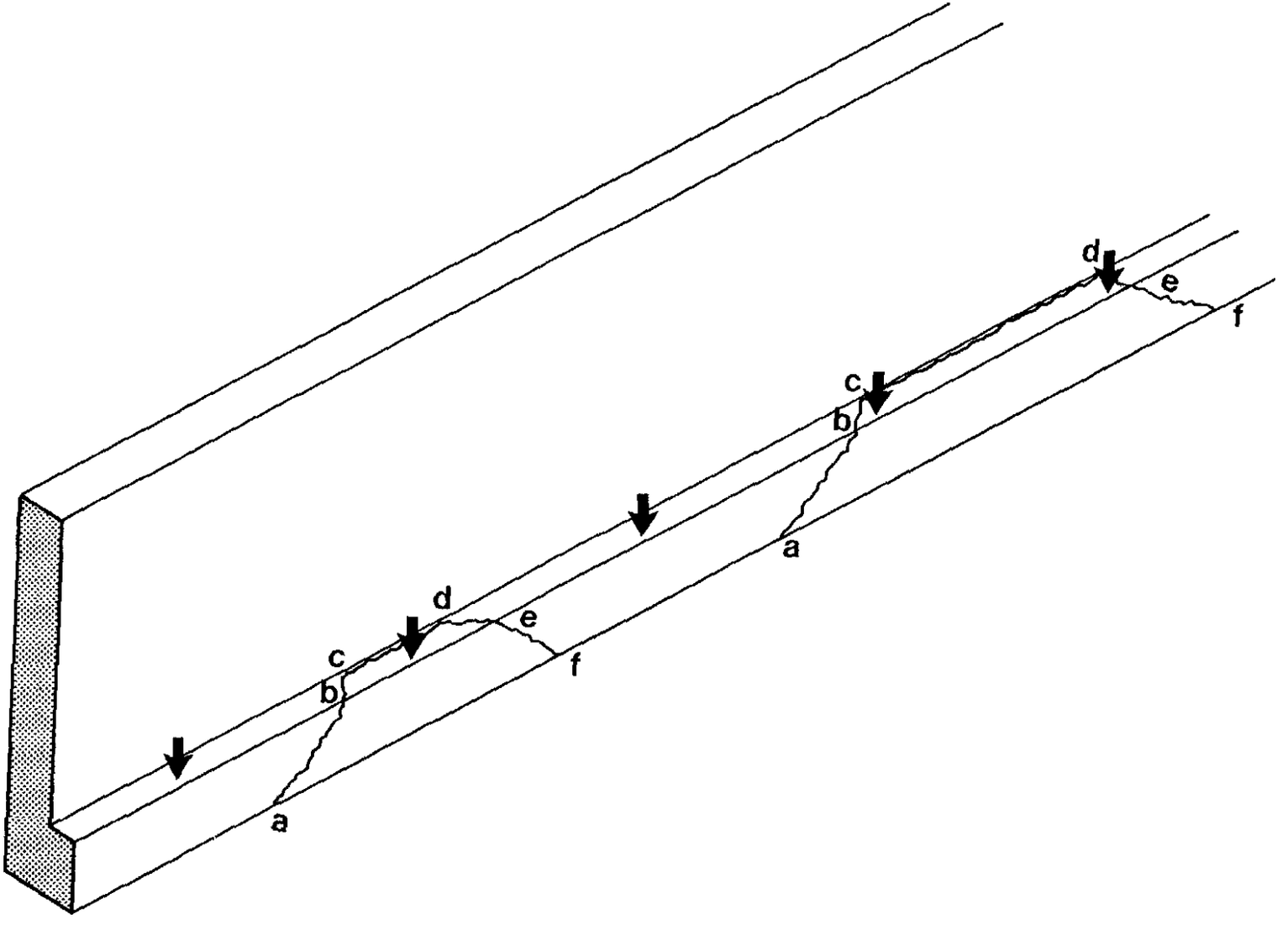

Fig. 5.6 - Local failures related to punching shear strength of ledge

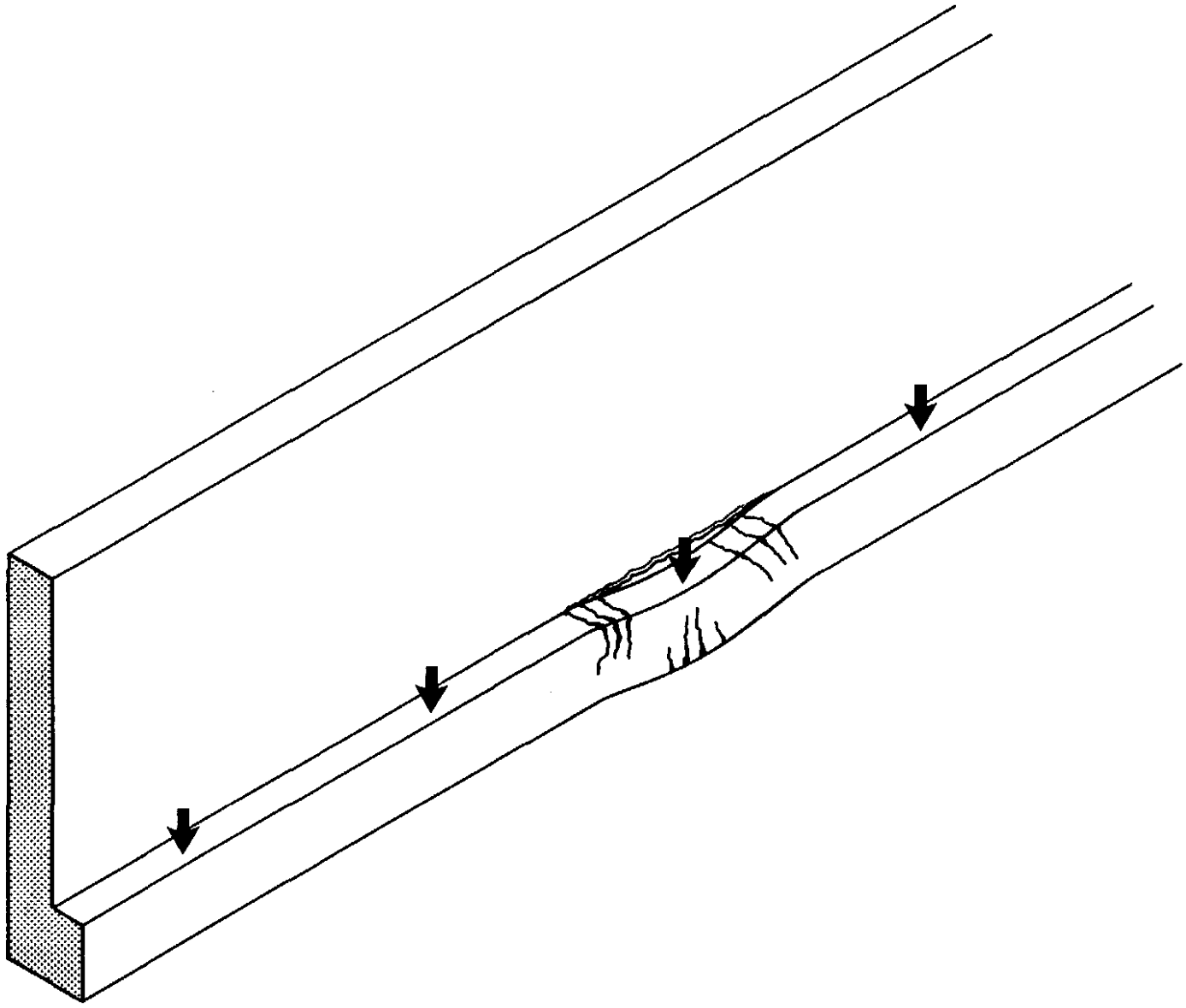

Fig. 5.7 - Local hanger reinforcement failure related to bending strength of ledge

6. FINDINGS AND RECOMMENDATIONS

The following paragraphs describe the findings based on the background research. analytical studies, and load tests described herein.

- Critical section. Because spandrel beams are loaded "ear the bottom, a critical section for shear and torsion at the face of the support should be considered.
- Influence of deck connections. Connections to deck **elements** do not substantially reduce torsion, however, they are effective in restraining lateral displacement induced by bending about the weak principal axis.
- Shear and torsion of prestressed L-beams. Methods which consider a concrete contribution for shear and torsion design of prestressed spandrels, such as the Zis-McGee or the Zia-Hsu methods, have been verified by two tests. Design methods based on compression field theory are somewhat more conservative, particularly with regard to the requirement for negative bending strength at the face of the support.
- Shear strength of pocket spandrels. An approach for considering the effect of the pocket on the shear strength of pocket spandrels has been proposed. While the accuracy of this approach has not been fully verified by tests, it is believed to be conservative.
- Detailing practices. The torsional response of deep spandrels is dominated by out-of-plane bending. The use of lapped-splice stirrups and longitudinal reinforcing bars without hooks does not appear to have any detrimental effect.
- Beam end design. Two independent design checks in the end region of spandrels are recommended. First, reinforcement should be provided to resist out-of-plane bending caused by the horizontal torsional equilibrium reactions. This reinforcement is not additive to the reinforcement for internal torsion. and very little supplemental steel will be required provided a

critical section for shear and torsion at the face of the support is considered. Second, the developed force in the primary longitudinal reinforcement at the face of the support, or bottom corner of a dapped-end connection. should equilibrate the applied normal force, as well as the axial force induced by the vertical reaction.

- Ledge hanger reinforcing. The eccentricity of the ledge load cannot be neglected in design of hanger reinforcement for ledge-to-web attachment. Nonetheless, not all of the load acting on the ledge is suspended from the web and the effective eccentricity of the ledge load is significantly reduced due to torsion within the ledge. A design procedure which considers these effects has been recommended. Load tests conducted under this program and by others have verified this procedure. In addition, it was determined that hanger reinforcement is not additive to shear and torsion reinforcement. Minimum hanger reinforcement amounts are recommended and distribution of ledge reinforcing is discussed.
- Ledge punching shear. PCI design equations for the punching shear strength of beam ledges may be unconservative. Further research in this area is recommended.

In closing, it should be reemphasized that this study has focused on spandrel beams as load-carrying components. In this regard, the research has gone a long way toward the understanding and resolution of several fundamental aspects of spandrel beam design. The findings generally apply to both prestressed and conventionally-reinforced spandrels commonly used in buildings and parking structures. However, forces from frame action, volume change. handling and vehicular impact were not discussed, and the report does not fully address tolerances, corrosion protection or connection details. These factors must also be carefully considered during the design process.

ACKNOWLEDGEMENTS

Throughout the study, the Steering Committee for PCISFRAD Project #5 provided helpful guidance and perspective. In particular, Ned Cleland, Alex Aswad, and Kamal Chaudhari contributed significantly through their constructive comments.

The support of Wiss, Janney, Elstner Associates, Inc. in conducting this research is gratefully acknowledged. The author would like to specifically thank John Hanson, John Fraczek, Lilia Glikin, Dirk Heidbrink. and Doris Nelson for the assistance.

The test specimens were fabricated by J. W. Peters. Their performance in this difficult and precise task is a credit to their talent as a precast producer.

Also, the author wishes to express his appreciation to Susan Klein of Susan Klein Graphic Design for her help in preparation of the graphic figures.

Finally, this research was funded by the PCI Specially Funded Research and Development Program. The author wishes to thank the administrators and contributors to that program who made this research possible.

NOTATION

a	=	shear span, distance between concentrated load or reaction and hanger reinforcement
A_s	=	area of flexural tension reinforcement
A_{sh}	=	area of hanger reinforcing
$A_{s\ell}$	=	area of reinforcement in the top or bottom of the ledge in addition to the reinforcement required for the primary moment
A_v	=	area of shear reinforcement
$A_{w\ell}$	=	area of longitudinal web-reinforcement for bending due to torsional equilibrium reactions
A_{wv}	=	area of vertical web reinforcement for bending due to torsional equilibrium reactions
b	=	bearing width of concentrated ledge load
b_a	=	width of ledge measured along the bottom of the beam
b_o	=	perimeter of critical section
b_w	=	web width
c	=	distance from extreme fiber to neutral axis
d	=	distance from extreme compression fiber to centroid of flexural tension reinforcement
d_ℓ	=	effective depth of ledge reinforcing
e	=	distance from centerline web to ledge load
e_ℓ	=	distance from centroid of critical section for shear to ledge load
f'_c	=	compressive strength of concrete, psi
$\sqrt{f'_c}$	=	square root of compressive strength of concrete, psi
f_{sd}	=	developed stress in primary flexural reinforcement
f_Y	=	yield strength of reinforcement
f_u	=	ultimate tensile strength of reinforcement
h	=	overall height of section
h_ℓ	=	height of ledge

h_p = height of pocket in pocket spandrel

h_s = height of beam effective in resisting bending due to
= torsional equilibrium reactions

j = ratio of internal moment arm to total effective depth

J_c = property of critical section analagous to polar moment of inertia

N_u = axial force at bearing

s = spacing of shear or torsion reinforcing

s = spacing of ledge loads

T_c = torsional moment strength provided by concrete

T_ℓ = torsional moment in ledge

T_u = factored torsional moment at critical section

v_c = shear strength provided by concrete

V_ℓ = shear in ledge

V_u = factored shear force

V_u = factored reaction

x = shorter overall dimension of a rectangular cross section

Y = longer overall dimension of a rectangular cross section

A = symbol for difference

γ_t = reduction factor for torsion in ledge

ϕ = capacity reduction factor

Σ = summation symbol

REFERENCES

1. Building Code Requirements for Reinforced Concrete (ACI 318-83), American Concrete Institute, Detroit, MI.

2. MacGregor, James G.. Chmn., "The Shear Strength of Reinforced Concrete Members, by the Task Committee on Masonry and Reinforced Concrete of the Structural Division," Journal of the Structural Division, ASCE, Vol. 99, No. ST6, Proc. Paper 9791, June 1973, pp. 1091-1187.

3. PCI Design Handbook, Third Edition, Prestressed Concrete Institute, Chicago, IL, 1985.

4. Notes on ACI 318-83, Portland Cement Association, Fourth Edition, 1984. pp. 14-28.

5. Cleland, Ned M.. "Identification of Secondary Behavior in Combined Bending, Shear, and Torsion of Reinforced Concrete Ledger Beams," Ph.D Dissertation, University of Virginia School of Engineering and Applied Science, August, 1984.

6. Iverson, James K. and Pfeifer, Donald W., "Bearing Pads for Precast Concrete Buildings," PCI Journal, V. 30, No. 5, September-October 1985, pp. 128-154.

7. Zia, Paul and McGee. W. Denis, "Torsion Design of Prestressed Concrete," Journal of the Prestressed Concrete Institute, Vol. 19, No. 2, March-April 1974, pp. 46-65.

8. PCI Design Handbook, Second Edition, Prestressed Concrete Institute, Chicago, IL, 1978.

9. Zia , Paul and Hsu. Thomas, "Design for Torsion and Shear in Prestressed Concrete," Preprint 3424, ASCE Chicago Exposition, October, 1978.

10. Raths, Charles H.. "Spandrel Beam Behavior and Design," PCI Journal. Vol. 29. No. 2. March-April 1984, pp. 62-131.

11. Osborn. Andrew E. N., "Design of Ledger Girders," Draft report for PCI Connection Details Committee, April 1984.

12. Collins, Michael P.. and Mitchell, Denis, "Shear and Torsion Design of Prestressed and Non-Prestressed Concrete Beams," PCI Journal, Vol. 25. September-October 1980, pp. 85-86.

13. Sturm, Edward R., "Theory of Deflection Compatibility," Private correspondence to Andrew Osborn. May 1984.

REFERENCES (continued)

14. Mirza, Sher Ali, and Furlong, Richard W., "Serviceability Behavior and Failure Mechanisms of Concrete Inverted T-Beam Bridge Bentcaps." ACI Journal, Proceedings Vol. 80, No. 4. July-August 1983, pp. 294-304.

15. Krauklis, A. T. and Guedelhofer, 0. C., Comments on "Spandrel Beam Behavior and Design." (Ref. 10), PCI Journal, V. 30, No. 5, September-October 1985. pp. 171-174.

16. Hanson, John M., "Square Openings in Webs of Continuous Joists." PCA Research and Development Bulletin, Portland Cement Association, 1969, 14 PP.

17. Rice, Paul F., et al, Structural Design Guide to the ACI Building Code, Third Edition, Van Nostrand Reinhold Co., Inc., New York, NY, 1985. 477 pp.

APPENDIX A – SPANDREL DESIGN CHECKLIST

General

The following checklist items are presented in an order of their usual consideration in the design process. which is not necessarily the order of importance. Some of these design considerations are illustrated in Appendices B and C, however, due to the limited scope of research under PCISFRAD Project #5, many of the items listed below are not addressed. The reader is directed to the appropriate section of the PCI Handbook and Reference 10 for discussion of design considerations outside the scope of this research.

Dimensions

- Span
- Web height and width
- Ledge depth and projection
- Daps and blockouts

Loads

- Dead and live
- Frame action
- Volume change
- Vehicular impact

Flexure

- Service load stresses:
  - at release
  - in service
- Flexural strength
- Minimum reinforcement
- Out-of-plane bending:
  - during handling
  - during erection
  - due to vehicular impact
- Sweep due to strand eccentricity
- Principal axis analysis for slender L-beams

Shear and Torsion

- Eccentricity contributing to torsion
- Minimum and maximum torsion
- Transverse reinforcement
- Longitudinal reinforcement

Beam End Design

- Torsion equilibrium reinforcement
- Longitudinal reinforcement at end
- Beam bearing design
- Dapped end design

Ledge Design

- Tee stem bearing
- Punching shear:
  - at interior reaction
  - at outside reaction
- Ledge flexure
- Hanger reinforcement
- Ledge distribution reinforcement

Details

- Column and deck connections
- Reinforcement details:
  - anchorage/development
  - spacing
  - tolerance and clearance
- Corrosion protection:
  - concrete cover
  - protection of exposed plates
  - protection of end of strand
- Inserts for handling

APPENDIX B
EXAMPLE 1 - L-BEAM FOR PARKING STRUCTURE

DESIGN LOADS

STEM REACTIONS

DEAD LOAD (90 PSF) = 0.09(60/2)4 = 10.8 kips
LIVE LOAD (50 PSF) = 0.05(60/2)4 = 6.0 kips

TOTAL SERVICE LOAD = 16.8 kips

FACTORED LOAD = 1.4x10.8 + 1.7x6.0 = 25.3 kips

EQUIVALENT UNIFORM LOAD

SERVICE: $w = 16.8/4 + 0.675 = 4.88$ k/ft
FACTORED: $w_u = 25.3/4 + 1.4x0.675 = 7.27$ k/ft

BASIC UNIFORM LOADS ARE INCREASED BY RATIO OF GRID SPAN TO DESIGN SPAN. GRID SPAN = 28.0 ft. SHEAR SPAN = 27.0 ft.

SERVICE (ADJUSTED): $w = 4.88 \times 28/27 = 5.06$ k/ft
FACTORED (ADJUSTED): $w = 7.27 \times 28/27 = 7.54$ k/ft

FLEXIJRE

THE FOLLOWING IS A SUMMARY OF THE FLEXURE DESIGN. REFER TO PCI HANDBOOK SECTION 4.2 FOR DETAILS OF THE DESIGN PROCEDURE.

SERVICE LOAD MOMENT = 5533 in-k

NOTE: THE MOMENT COMPUTED USING THE ADJUSTED EQUIVALENT UNIFORM LOAD IS ABOUT 2% GREATER THAN THE VALUE COMPUTED USING CONCENTRATED LOADS.

PRESTRESS: 4 1/2 in. DIAMETER STRAND $y_{ps} = 5.0$ in.

	At Release (7% Loss)		In Service (17% Loss)			
	f_b	f_t	f_b	f_t	f_{pc}	f_{pe}
COMPUTED(psi)	483	-215	-166	525	148	430
ALLOW.(psi)	2100	-355	-424	2250		

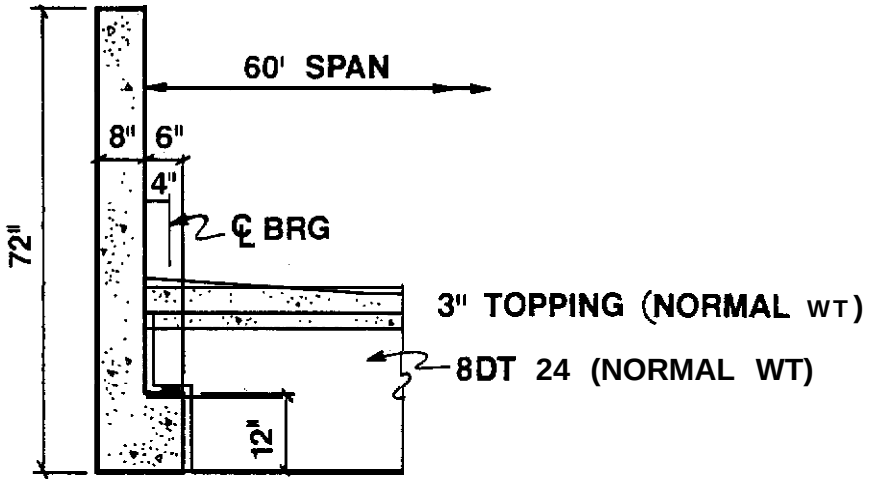

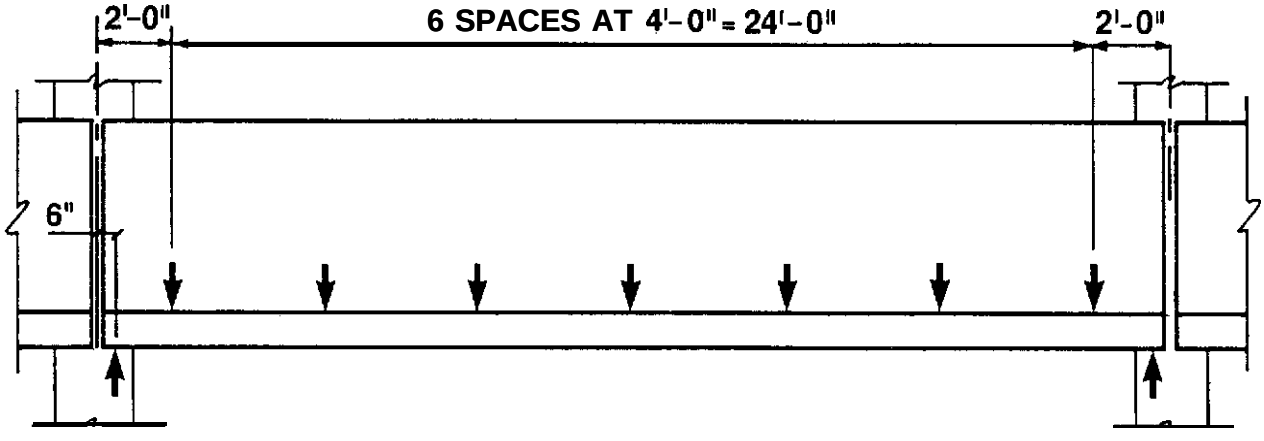

DESIGN DATA

f'_c = 5000 psi
f'_{ci} = 3500 psi
f_Y = 60 ksi
$f_{p"}$ = 270 ksi
(1/2" dia. stress relieved strand)
Clearance to stirrups = 1 1/4"

SECTION PROPERTIES

A = 648 in^2
I = 307,296 in^4
Y = 32.67 in
Z_b = 9406 in^3
Z_t = 7813 in^3
WT = 0.675 k/ft

Fig. B1 – L-beam geometry and design data

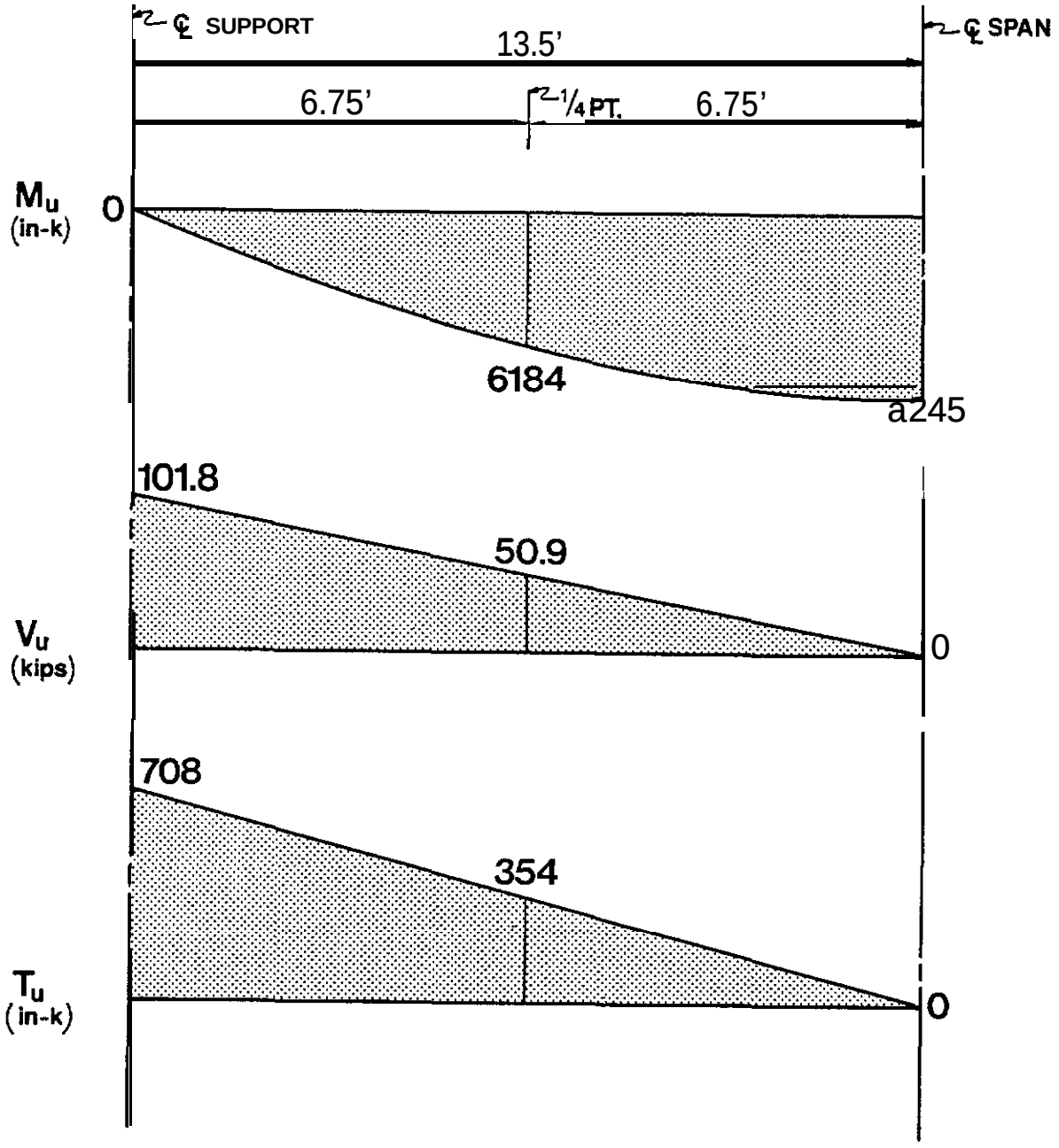

Fig. B2 - Moment, shear and torsion diagrams

ULTIMATE STRENGTH:

A_{ps} = 0.612 in.^{2} A_s = 4-#4 = 0.80 in.^{2}

M_n = 9243(prestress) + 2654(mild reinf.) = 11,897 in-k

M_u = 8245 in-k < 11,897 in-k

$1.2M_{cr} = 1.2(7.5\sqrt{f'_c}+f_{pe})Z_b = 1.2(7.5\sqrt{5000}+430)9406/1000$

= 10.840 in-k < 11.897 in-k

SHEAR AND TORSION

THE SHEAR AND TORSION DESIGN FOLLOW THE ZIA-HSU METHOD (REF. 9). SEE FIG. B2 FOR BENDING SHEAR AND TORSION DIAGRAMS.

SHEAR AND TORSION PROPERTIES OF SECTION

	x	y	x^2y
WEB (ABOVE LEDGE)	8	60	3840
LEDGE	12	14	2016
		Σx^2y	5856

$b_w d = 8x66.6 = 533$ in^2

$C_t = b_w d/\Sigma x^2y = 5353/5856 = 0.091/\text{in}^{-1}$

MINIMUM TORSION

$\gamma_t = \sqrt{1 + 10f_{pc}/f'_c} = \sqrt{1 + 10x148/5000} = 1.14$

$T_{min} = \phi(0.5\sqrt{f'_c}\gamma_t\Sigma x^2y)$

= 0.85(0.5$\sqrt{5000}$x1.14x5856 = 201 in-k < 708 in-k

THEREFORE, TORSION DESIGN IS REQURIED.

MAXIMUM TORSION

$c = 12 - 10(f_{pc}/f'_c) = 12 - 10(148/5000) = 11.7$

$$T_{max} = \frac{(1/3)C\gamma_t\sqrt{f'_c}\Sigma x^2 y}{\sqrt{1+(C\gamma_t V_u/30C_t T_u)}} = \frac{(1/3)11.7x1.14\sqrt{5000}x5856}{\sqrt{1+(11.7x1.14x101.8/(30x0.091/x708)}}$$

$= 1540$ in-k > 708 in-k ok

SHEAR AND TORSION STRENGTH OF CONCRETE

AT SUPPORT:

$$V'_c = V_{cw} = (3.5\sqrt{f'_c} + 0.3f_{pc})b_w d + V_p$$

$= (3.5\sqrt{5000}+0.3x0)8x66.8 + 0 = 131{,}900$ lbs $= 131.9$ kips $< V_{ci}$

NOTE: STRAND IS NOT DEVELOPED AT SUPPORT, THEREFORE, $f_{pc} = 0$ and $\gamma_t = 1.0$.

$$T'_c = 2\sqrt{f'_c}\Sigma x^2 y\ (\gamma_t - 0.6)$$

$= 2\sqrt{5000}x5856(1.0-0.6) = 331{,}000$ in-lbs $= 331$ in-k

$$V_c = V'_c/\sqrt{1 + [(V'_c T_u)/(T'_c V_u)]^2}$$

$$= 131.9/\sqrt{1 + [(131.9x708)/(331x101.8)]^2} = 44.8 \text{ kips}$$

$$T_c = T'_c/\sqrt{1 + [(T'_c V_u)/(V'_c T_u)]^2}$$

$$= 331/\sqrt{1 + [(331x101.8)/(131.9/708)]^3} = 311 \text{ in-k}$$

AT QUARTER POINT:

$$M_{cr} = Z_b\ (6\sqrt{f'_c}+f_{pe}) = 9406(6\sqrt{5000}+430)/1000 = 8035 \text{ in-k}$$

$$V'_c = V_{ci} = 0.6\sqrt{f'_c}\ b_w d + V_u M_{cr}/M_u$$

$= 0.6\sqrt{5000}x8x66.6/1000 + 50.9x8035/6184$

$= 88.7$ in-k

$$T'_c = 2\sqrt{5000}x5856(1.14-0.6)/1000 = 447 \text{ in-k}$$

$$V_c = 88.7/\sqrt{1 + [(88.7x354)/(447x50.9)]^2} = 52.0 \text{ in-k}$$

$$T_c = 447/h\overline{ + [(447x50.9)/(88.7x3540]^2} = 362 \text{ in-k}$$

TRANSVERSE REINFORCEMENT

AT SUPPORT:

$A_v/s = (V_u/\phi - V_c)/df_y = (101.8/0.85-44.8)/(66.6x60)$

$= 0.019\ in^2/in. = 0.23\ in^2/ft$

$T_s = T_u/\phi - T_c = 708/0.85 - 311 = 522$ in-k

$\alpha_t = 0.66 + 0.33y_1/x_1 \leq 1.5 = 0.66 + 0.33x69/5 = 5.2.\ a_t = 1.5$

$A_t/s = T_s/\alpha_t x_1 y_1 f_y = 522/(1.5x5x69x60) = 0.017\ in^2/in$

$= 0.20\ in^2/ft$

$(A_v + 2A_t)/s = 0.23 + 2x0.20 = 0.63\ in^2/ft$

Min $(A_v + 2A_t)/s = 50(b_w/f_y)(1 + 12\ f_{pc}/f'_c) \leq 200\ b_w/f_y$

$= 50(8/60,000)(1+12x148/5000) = 0.009\ in^2/in$

$= 0.11\ in^2/ft$

SEE "BEAM END DESIGN" FOR SELECTION OF REINFORCEMENT.

AT QUARTER POINT:

$A_v/s = (50.9/0.85 - 52.0)/(66.6x60) = 0.002\ in^2 = 0.02\ in^2/ft$

$T_s = 354/0.85 - 362 = 54$ in-k

$A_t/s = 54/(1.5x5x69x60) = 0.002\ in^2/in = 0.02\ in^2/ft$

$(A_v + 2A_t)/s = 0.02 + 2x0.02 = 0.06\ in^2/ft$

Min $(A_v + 2A_t)/s = 0.11\ in^2/ft$ (CONTROLS)

Use #3 at 12: $0.11\ in^2/ft$

LONGITUDINAL REINFORCEMENT

$A_\ell = (2A_t/s)(x_1 + y_1)$ or Ref 9. Eq 7

$$A_\ell = \left[440x \frac{T_u}{f_y} \frac{}{T_u + V_u/3C_t} - 2A_t/s \right] (x_1 + y_1)$$ Ref 9, Eq 8

WHICHEVER IS GREATER, WHERE

$2A_t/s$ (IN EQ 8) $\geq 50b_w \leq (1+12f_{pc}/f'_c) = 0.009\ in^2/in.$

	$2A_t/s$ (in^2/in)	A_ℓ (Eq 7) (in^2)	T_u (in-k)	V_u (kips)	A_ℓ (Eq 8) (in^2)	A_ℓ (in^2)
AT SUPPORT:	0.034	2.52	708	101.8	0.05	2.52
AT QUARTER PT:	0.002	0.15	354	50.9	1.90	1.90

USE 7-#4 EACH SIDE OF WEB, $A_\ell = 2.80\ in^2$

BEAM END DESIGN

TORSION EQUILIBRIUM REINFORCEMENT

$d_s = 8 - 1.25 - 0.5 = 6.25$ in.: $h_s = 72 - 12 - 6 = 54$ in.

$$A_{WY} = A_{w\ell} = \frac{T_u}{2\phi f_y d_s} = \frac{708}{2x0.85x60x6.25} = 1.11\ in^2$$

$A_{wv}/h_s = 1.11/54 = 0.021/in^2/in. = 0.25\ in^2/ft$

$A_t/s = 0.20\ in^2/ft$ (SHT B6), THEREFORE, A_{wv}/s CONTROLS

$(A_v + 2A_{wv})/s = 0.23 + 2x0.25 = 0.76\ in^2/ft$

USE #4 STIRRUPS AT 6 in. $= 0.80\ in^2/ft$

6-#4 IN. WEB ABOVE LEDGE, $A_{w\ell} = 1.20\ in^2 > 1.11\ in^2$

THEREFORE, SPECIFIED A_ℓ REINFORCEMENT IS ADEQUATE.

REINFORCED CONCRETE BEARING

BASED ON SECTION 6.9 OF THE PCI HANDBOOK, $A_{vf} + A_n = 1.02\ in^2$

2-#7 BARS WELDED TO BEARING PLATE PROVIDED. REFER TO THE HANDBOOK FOR DETAILS OF THE DESIGN PROCEDURE.

LONGITUDINAL REINFORCEMENT AT END

$N_u = 0.2V_u = 0.2x101.8 = 20.4$ kips

$a = 5 + (h-d) = 5 + (72-66.6) = 10.4$ in.

$$\phi A_s f_{sd} = N_u h/d + V_u(0.5 + a/d)$$

$$= 20.4x72/66.6 + 101.8(0.5 + 10.4/66.6) = 88.9 \text{ kips}$$

BARS	DEVELOPED STRESS	ϕ x DEVELOPED FORCE
4 - #4	60x8/12 = 40 ksi	0.9x40x0.8 = 28.8
4 - 1/2 in. STRAND	150x10/25 = 60 ksi	0.9x60x0.61 = 32.9
2 - #7 (WELDED TO BRG PLATE)	60 ksi	0.9x60x1.20 = 64.8
		126.5 kips ok

LEDGE DESIGN

BEARING, PUNCHING SHEAR & LEDGE FLEXURE

THE FOLLOWING IS A SUMMARY OF THE LEDGE DESIGN FOLLOWING PCI HANDBOOK PROCEDURES. REFER TO PART 6 OF THE HANDBOOK FOR DETAILS OF THE DESIGN PROCEDURE.

BEARING: BEARING REINFORCEMENT IS NOT REQUIRED.

PUNCHING SHEAR: PUNCHING SHEAR STRENGTH IS ABOUT TWICE THE 25.3 kip STEM REACTION (THEREFORE, APPARENT INACCURACY OF PCI EQUATIONS IS NOT A CONCERN. ALSO, THE 42.7 kip TEST RESULT IS MUCH GREATER THAN THE STEM REACTION).

LEDGE FLEXURE: $A_s = 0.50$ in.^{2} DISTRIBUTED EVENLY BETWEEN STEM REACTIONS. USE #4 AT 12 in.; A, = 0.80 in^2.

HANGER REINFORCEMENT

$V_u = 25.3$ kips

$AV_a = V_u(3-2h_\ell/h)(h_\ell/h)^2 = 25.3(3 - 2x12/72)(12/72)^2 = 1.9$ kips

$\gamma_t = T_c/T_u = 311/708 = 0.44$

$\Delta T_\ell = V_u e \gamma_t (x^2y)_{ledge}/\Sigma x^2 y = 25.3x8x0.44x2016/5856 = 30.7$ in-k

d = 8 - 1.25 - 0.25 = 6.5 in.: a = 4 + 1.25 + 0.25 = 5.5 in.

$A_{sh} = [V_u(d + a) - \Delta V_\ell b_\ell/2 - \Delta T_\ell]/(\phi f_y d)$

$= [25.3(6.5+5.5) - 1.9x14/2 - 30.7]/0.85x60x6.5 = 0.78$ in^2

NEAR SUPPORT: (#4 STIRRUPS AT 6 in., 3 ft TRIB. LENGTH AT END)

$A_{sh} = 0.4$ in^2/ft (3 ft) = 1.20 in^2

MIDSPAN: ADD #3 ⌊ AT 12; ALTERNATE WITH #3 STIRRUPS AT 12

$A_{sh} = 2x0.11x4 = 0.88$ in^2

MINIMUM: $A_{sh} = 100\ sd/f_Y = 100x48x6.5/60,000 = 0.52$ in^2

TRANSVERSE REINFORCEMENT SUMMARY (INSIDE FACE in^2/ft)

		NEAR SUPPORT	MIDSPAN
SHEAR/TORSION	$(0.5A_v + A_t)/s$	0.32	0.11 (MIN)
TORSION EQUIL.	$(0.5A_v + A_{wv})/s$	0.38	
HANGER REINF.	A_{sh} (per ft)	0.26	0.20
PROVIDED		x4 at 6 (0.40)	#3 at 6 (0.22)

LEDGE DISTRIBUTION REINFORCING

PUNCHING SHEAR STRENGH IS ADEQUATE, THEREFORE, ALL HANGER REINFORCEMENT AND LEDGE FLEXURE REINFORCEMENT BETWEEN LEDGE LOADS ARE CONSIDERED EFFECTIVE, PROVIDED FLEXURAL STRENGTH OF LEDGE IS ADEQUATE.

$d_\ell = 12 - 3 = 9$ in.

$A_{s\ell} = V_u s/8\phi d_\ell f_y = 25.3x48/(8x0.85x9x60) = 0.33\ in^2$

THE 2-#4 BARS AT THE END OF THE LEDGE ARE NOT REQUIRED FOR THE BASIC FLEXURAL MOMENT. (THEY ARE NEEDED TO HELP RESIST $1.2\ M_{cr}$), THEREFORE THEY MAY BE CONSIDERED AS $A_{s\ell}$ REINFORCEMENT.

APPENDIX C

EXAMPLE 2 – POCKET SPANDREL FOR PARKING STRUCTURE

GENERAL

THIS EXAMPLE ILLIJSTRATES DESIGN OF SHEAR, END REGION, AND HANGER REINFORCEMENT FOR A DAPPED POCKET SPANDREL. NOTE THAT A POCKET IS PROVIDED NEAR THE DAPPED END. OFTEN THIS POCKET IS OMMITTED DUE TO DETAILING DIFFICULTIES (A WELDED BRACKET OR CAZALY HANGER IS USED, INSTEAD). SHEAR AND BENDING FORCES ARE IDENTICAL TO THOSE IN EXAMPLE 1 (FIG. B2). REFER TO FIG. Cl FOR FRAMING DETAILS AND DESIGN DATA.

IN ADDITION, THE FOLLOWING IS GIVEN:

f_{pc} = 167 psi, f_{pe} = 904 psi (AT POCKET), d = 67.0

SHEAR AND TORSION

TORSION AT SUPPORT

STEM REACTION = 25.3 kips; e = 2.0 in.

$T_u = 7 \times 25.3 \times 2.0/2 = 177$ in-k

INSIDE OUTER REACTION: $T_u = 5 \times 25.3 \times 2.0/2 = 127$ in-k

MINIMUM TORSION

$\gamma_t = \sqrt{1 + 10 f_{pc}/f'_c} = \sqrt{1 + 10 \times 167/5000} = 1.15$

$\Sigma x^2 y = 8^2 \times 72 = 4608$

$T_{min} = \phi(0.5\sqrt{f'_c}\gamma_t \Sigma x^2 y)$

$= 0.85 \times 0.5\sqrt{5000} \times 1.15 \times 4608/1000 = 159$ in-k

THEREFORE, TORSION DESIGN NOT REQUIRED INSIDE OUTER REACTION. DESIGN END REGION FOR TORSION EQUILIBRIUM REACTIONS AT SUPPORTS.

SHEAR STRENGTH OF CONCRETE

AT SUPPORT:

$V_c = V_{cw} = (3.5\sqrt{f'_c} + 0.3 f_{pc}) b_w (d - h_p)$

$= (3.5\sqrt{5000} + 0) 8 (67.0 - 24.0)/1000 = 85.1$ kips

AT QUARTER POINT (SEE ART 11.4.2 OF ACI 318-83 COMMENTARY):

$M_{cr} = Z_b (6\sqrt{f'_c} + f_{pe}) = 5023(6\ 5000 + 904)/1000$

$= 6672$ in-k (AT POCKET)

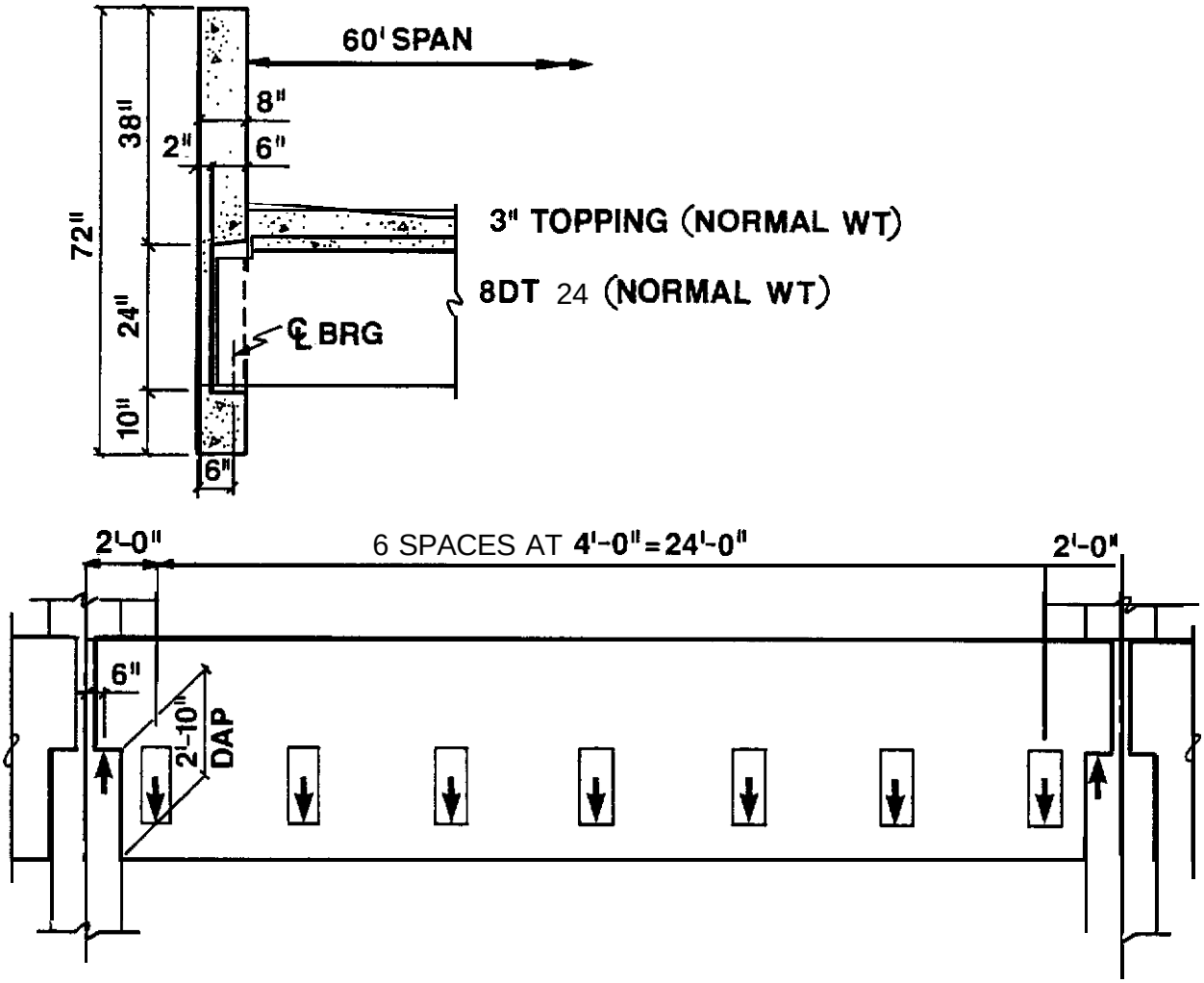

DESIGN DATA		FULL SECTION	AT POCKET
f'_c = 5000 psi	AREA	576 in^2	432 in^2
f'_{ci} = 3500 psi	I	248,832 in^4	204.288 in^4
f_y = 60 ksi (bars)	y_b	36.0 in	40.7 in
f_y = 70 ksi (WWF)	Z_b	6912 in^3	5023 in^3
$f_{p"}$ = 270 ksi	Z_t	6912 in^3	6520 in^3

Fig. Cl - Pocket spandrel geometry and design data

$V_c = V_{ci} = 0.6\sqrt{f'_c} b_w (d-h_p) + V_u M_{cr}/M_u$

$= 0.6\sqrt{5000} x8(67.0-24.0)/1000 + 50.9x6672/6184$

$= 69.5 \text{ kips} < V_u$

SHEAR REINFORCEMENT

$A_v/s = (V_u/\phi - V_c)/(d-h_p)f_Y$

$= (101.8/0.85-85.1)/(67.0-24.0)60 = 0.013 \text{ in}^2/\text{in.}$

$= 0.16 \text{ in}^2/\text{ft}$

MIN $A_v/s = 50b_w/f_Y = 50x8/60{,}000 = 0.0067 \text{ in}^2/\text{in.} = 0.080 \text{ in}^2/\text{ft}$

USE 1 LAYER 12x6-W2.0xW4.0 EACH FACE, FULL LENGTH

$A_v/s = 2x0.08 = 0.16 \text{ in}^2/\text{ft}$

BEAM END DESIGN

TORSION EQUILIBRIUM REINFORCEMENT

$d_s = 8.0 - 1.5 = 6.5 \text{ in.}$

$A_{wv} = A_{w\ell} = T_u/2\phi f_y d_s = 177/(2x0.85x70x6.5) = 0.23 \text{ in}^2$

$h_s = 38 - 6 = 32 \text{ in.}$

$A_{wv}/s = A_{w\ell}/s = 0.23/32 = 0.0072 \text{ in}^2/\text{in.} = 0.086 \text{ in}^2/\text{ft}$

ASE ADD'L LAYER 6x6-W4.0xW4.0 INSIDE FACE, EACH END.

$A_{wv}/s = A_{w\ell}/s = 0.08 \text{ in}^2/\text{ft}$

DAPPED END DESIGN

DAPPED END DESIGN IS BASED ON THE END DETAIL AND EQUILIBRIUM FORCE MODELS SHOWN IN FIG. C2. IT SHOULD BE NOTED, HOWEVER, THAT THE REINFORCEMENT SCHEME AND DESIGN PROCEDURE HAVE NOT BEEN VALIDATED BY LOAD TESTS.

DIRECT SHEAR (SEE PCI ARTICLE 6.13.2):

$\mu_e = 1000\lambda bh\mu/V_u \leq 3.4$

$= 1000x1x8x38x1.4/(101.8x1000) = 4.18 \rightarrow \mu_e = 3.4$

$A_n = N_u/(\phi f_y) = 20.4/(0.85x60) = 0.40 \text{ in}^2$

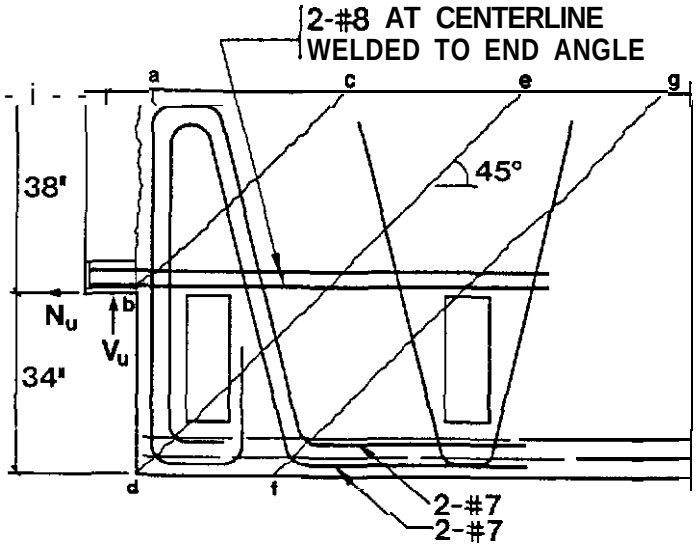

END DETAIL

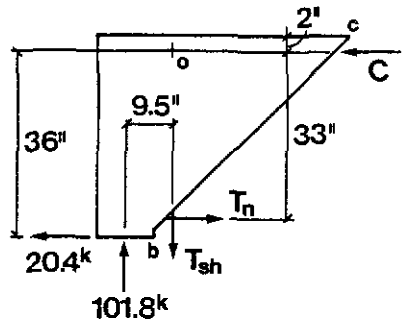

FORCE MODEL bc

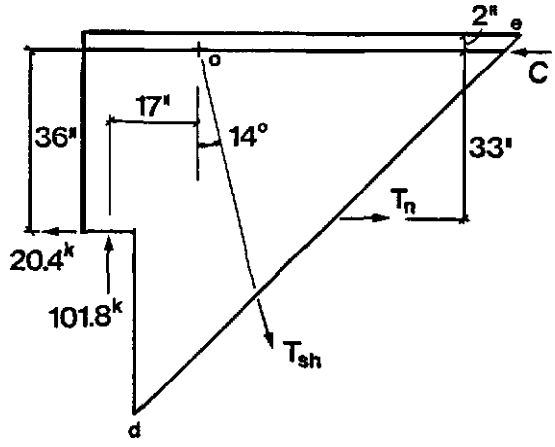

FORCE MODEL de

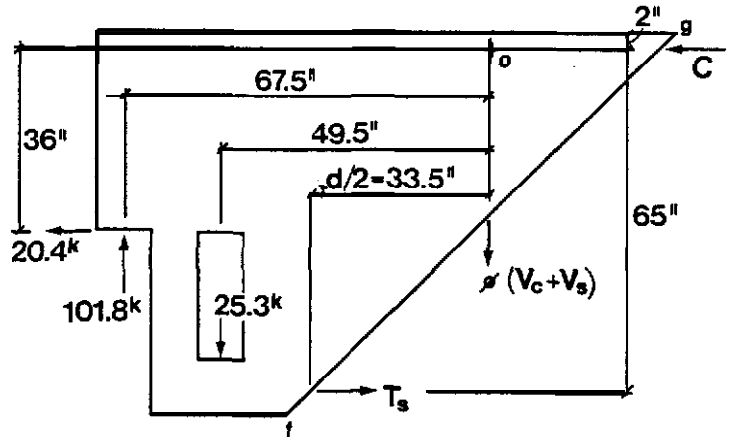

FORCE MODEL fg

Fig. C2 – Dapped end detail and force models

$A_s = 2V_u/(3\phi f_y \mu_e) + A_n$

$= 2x101.8/(3x0.85x60x3.4) + 0.40 = 0.79\ in^2$

2-#8 PROVIDED: $A_s = 1.44\ in^2$

$Ah = 0.5(A_s - A_n) = 0.5(0.72-0.40) = 0.16\ in^2$

6x6-W4.0xW4.0 PROVIDED: $Ah = 3x0.08 = 0.24\ in^2$

CRACK AT RE-ENTRANT CORNER (FORCE MODEL bc):

NEGLECT INCLINED HANGER REINFORCEMENT

$\Sigma F_v = 0 \rightarrow T_{sh} = V_u = 101.8$ kips

$A_{sh} = T_{sh}/\phi f_Y = 101.8/(0.85x60) = 2.00\ in^2$

4-#7 PROVIDED; $A_{sh} = 2.40\ in^2$

$\Sigma M_o = 0 \rightarrow T_n = (20.4x36 + 101.8x9.5)/33 = 51.6$ kips

$A_n = T_n/\phi f_Y = 51.6/(0.85x60) = 1.01\ in^2$

2-#8 PROVIDED; $A_n = 1.58\ in^2$

CRACK AT BOTTOM CORNER (FORCE MODEL de):

NEGLECT VERTICAL HANGER REINFORCEMENT (NOT EFFECTIVE AT BEND).

$\Sigma F_v = 0 \rightarrow T_{sh} = V_u/\cos 14 = 101.8/\cos 14 = 104.9$ kips

$A_{sh} = 104.9/(0.85x60) = 2.06\ in^2$ (4-#7 ok)

$\Sigma M_o = 0 \rightarrow T_n = (20.4x36 + 101.8x17)/33 = 74.7$ kips

$A_n = 74.7/(0.85x60) = 1.46\ in^2$ (2-#8 ok)

FULL SECTION (FORCE MODEL fg):

HANGER REINFORCEMENT IS NOT EFFECTIVE DUE TO BEND.
NEGLECT A_n REINFORCEMENT

$CM_o = 0 \rightarrow T_s = (20.4x36 + 101.8x67.5 - 25.3x49.5)/65$

$= 97.7$ kips

PCI FIG. 4.10.4: f_{ps} = 170 ksi

$\phi A_{ps} f_{ps}$ = 0.9x0.61x170 = 93.3 kips SAY OK

CHECK DEPTH OF COMPRESSION BLOCK

$a = \Sigma F_h / 0.85 b f'_c$ = (97.7-20.4)/0.85x8x5 = 2.3 in

a/2 = 2.3/2 = 1.2 in < 2 in OK

HANGER REINFORCEMENT

AT POCKET

$A_{sh} = V_u / \phi f_y$ = 25.3/(0.90x60) = 0.47 in^2

USE 1-#4 $\sqcup$ 4 EA POCKET (PLUS 2-W4.0 WIRES)

A_{sh} = 2x0.20(cos14) + 2x0.04 = 0.47 in^2

$\ell_{dh} = 1200 d_b / \sqrt{f'_c}$ = 1200x0.5/$\sqrt{5000}$ = 8.5 in OK

Copyright © 1986
Prestressed Concrete Institute

All rights reserved. This book or any part thereof may not be reproduced in any form without the written permission of the Prestressed Concrete Institute.

This report is based an a research project supported by the PCI Specially Funded Research and Development (PCISFRAD) Program. The conduct of the research and the preparation of the final reports for each of the PCISFRAD projects were performed under the guidance of selected industry Steering Committees. It should be recognized that the research conclusions and recommendations are those of the researchers, and that the report was not subjected to the review and consensus procedures established for other W-published technical reports and documents. It is intended that the conclusions and recommendations of this reserach be considered by appropriate PCI technical committees and included. if viable. in future reports coming from these committees. In the meantime. this research report is made available to producers, engineers and others to use with appropriate engineering judgment similar to that applied to any new technical information.

ISBN 0-937040-30-4
Printed in U.S.A.

201 NORTH WELLS STREET
CHICAGO. ILLINOIS 60606
TELEPHONE: 312 f 346.4071

prestressed concrete institute